ENGINEERING RESEARCH INSTITUTE
THE UNIVERSITY OF MICHIGAN
ANN ARBOR

TECHNICAL REPORT TO JANUARY 1, 1958

INVESTIGATION OF NUCLEAR-ENERGY LEVELS

M. L. Wiedenbeck
Professor of Physics

ERI Project 2375

OFFICE OF NAVAL RESEARCH, U. S. NAVY DEPARTMENT
CONTRACT NO. Nonr-1224(13)
SPONSORING AGENCY PROJECT NO. NR024-015

January 1958

FOREWORD

Of the following seven articles, five are reprints of papers published in The Physical Review and the Bulletin of the American Physical Society during 1957 and 1958, and one has been accepted for publication by The Physical Review, and will probably appear in Volume 109 of that journal. The entire group of papers is submitted as a technical report for the year 1957.

The study of nuclear-energy levels is being continued both in the Physics Department of the University and at the Argonne National Laboratory, under their Participating University Program.

M. L. Wiedenbeck

M. L. Wiedenbeck

I

TRANSITION ENERGIES AND NUCLEAR LEVELS IN Sm^{152}, Sm^{154}, Gd^{152}, AND Gd^{154} AS DERIVED FROM THE SEPARATED ISOTOPES OF EUROPIUM

Reprinted from THE PHYSICAL REVIEW, Vol. 107, No. 6, 1621–1625, September 15, 1957
Printed in U. S. A.

Transition Energies and Nuclear Levels in Sm^{152}, Sm^{154}, Gd^{152}, and Gd^{154} as Derived from the Separated Isotopes of Europium*

J. M. CORK, M. K. BRICE, R. G. HELMER, AND D. E. SARASON
Harrison M. Randall Laboratory of Physics, University of Michigan, Ann Arbor, Michigan
(Received April 8, 1957)

Specimens of highly enriched Eu^{151} and Eu^{153} were irradiated in the Argonne CP-5 reactor and the product isotopes studied in both magnetic and scintillation spectrometers. Eu^{152} decays by electron emission to Gd^{152} and by K capture to Sm^{152}. Eu^{154} emits beta particles leading to Gd^{154} but no evidence appeared for positron emission or K capture leading to Sm^{154}. The many conversion-electron lines together with coincidence data allowed the evaluation of the gamma transitions and their arrangement in plausible nuclear level schemes. The beta spectra were resolved by the use of the double-focusing spectrometer. Each of the daughter nuclei is even-even in structure. A comparison is made of the observed lower energy transitions and the prediction from the "collective" model for rotational states.

NORMAL europium consists of two stable isotopes whose masses are 151 (47.8%) and 153 (52.2%). On neutron capture two long-lived radioactive isotopes of europium are produced. Many studies[1] have been made of these activities. Mass spectrometer analyses[2] of the active europium emitter showed it to be composed of two activities of nearly the same half-life. Spectrometer observations of the combined activity could not, except for a fortunate guess, lead to the correct assignment of the many gamma energies.

With the availability of the separated isotopes of europium the possibility of a proper interpretation of all observed conversion electron lines and gamma energies exists. A report[3] on the gamma energies derived from Eu^{152} as observed in a scintillation spectrometer has been presented. Eu^{152} can decay either by K capture to Sm^{152} or by beta emission to Gd^{152}. By using a scintillation crystal alone, the energies cannot be precisely evaluated nor is it possible with certainty to conclude in which of the final nuclei the transition occurs, except as this can be deduced from coincidence measurements.

In the present investigation enriched Eu^{151} (92%) and Eu^{153} (95%) were irradiated in the maximum flux of the Argonne reactor for one month. The resulting strong sources were studied in both magnetic photographic and scintillation spectrometers.

Some thirty well-defined electron lines whose energies are presented in Table I are observed for Eu^{152}. In addition, the energies of eight Auger electron lines have been evaluated, yielding values between 31.7 and 39.9 kev. It is apparent that certain groups of electron lines have energy differences characteristic of the electronic binding energies of samarium while other lines are better satisfied by the corresponding differences in gadolinium. The K-L difference for gadolinium is about 3 kev greater than for samarium, and since the energy of each electron line is good to about 0.2% a fairly certain conclusion can be made of the element in which each gamma transition occurs. When only a single electron line occurs, as is sometimes the case, the proper placement may be aided by coincidence observations with the scintillation spectrometer.

Similarly, the approximately twenty electron lines obtained with Eu^{154} are shown in Table II. Since the mass separation was not complete, there was some trace of each of the strong electron lines due to Eu^{152} when Eu^{154} was studied. These contamination lines are not recorded in the tables. The remarkable similarity between the spectra from the Eu^{152} and Eu^{154} sources for the energy band from 100 to 700 kev is shown in the reproduction of a composite spectrogram in Fig. 1.

Many of the electron lines for the two sources seem to have not only nearly the same energy but also

TABLE I. Conversion electron energies in kev and their interpretation for Eu^{152} (long-lived).

Electron energy	Interpretation	Energy sum	Electron energy	Interpretation	Energy sum
75.4	K Sm	122.3	567	K Sm	614
114.8	L_2 Sm	122.1		or K Gd	617
115.3	L_3 Sm	122.1	578.0	L Sm	585.7
120.5	M Sm	122.1	612.3	K Sm	659
122.0	N Sm	122.1		or K Gd	662
198.5	K Sm	245.3	645.0	K Sm	691.9
237.7	L Sm	245.4	684.2	L Sm	691.9
243.8	M Sm	245.4	731.8	K Gd	782.0
294.7	K Gd	345.1	773.8	L Gd	782.1
337.0	L Gd	345.1	825	K Sm	872
343.5	M Gd	345.2		or K Gd	875
362.2	K Gd	412.2	922	K Sm	969
398.3	K Sm	445.2	961	L Sm	969
	or K Gd	448.5	1045	K Sm	1092
404.3	L Gd	412.2	1071	K Sm	1118
456.9	K Gd	507.1	1111	L Sm	1119
498.1	L Gd	506.5	1369	K Sm	1416
539.0	K Sm	585.9	1408	L Sm	1416

* This investigation received the joint support of the Office of Naval Research and the U. S. Atomic Energy Commission.

[1] S. Ruben and M. Kamen, Phys. Rev. **57**, 489 (1940); Cork, Shreffler, and Fowler, Phys. Rev. **72**, 1209 (1947); see also Hollander, Perlman, and Seaborg, Revs. Modern Phys. **25**, 469 (1953); O. Nathan and M. Waggoner, Nuclear Phys. **2**, 548 (1957); F. S. Stephens, Jr., thesis, University of California, 1955 (unpublished).

[2] Karraker, Hayden, and Inghram, Phys. Rev. **87**, 901 (1952).

[3] L. Grodzins, Bull. Am. Phys. Soc. Ser. II, **1**, 163 (1956); H. Kendall and L. Grodzins, Bull. Am. Phys. Soc. Ser. II, **1**, 164 (1956).

TABLE II. Conversion electron energies in kev and their interpretation for Eu^{154}.

Electron energy	Interpretation	Energy sum	Electron energy	Interpretation	Energy sum
73.0	K Gd	123.2	675	K Gd	725
115.0	L Gd	123.1	686	L Gd	694
115.6	L_3 Gd	123.1	709	K Gd	759
121.2	M Gd	123.1	825	K Gd	875
122.5	N Gd	123.0		or K Sm	872
198.1	K Gd	248.3	949	K Gd	999
239.8	L Gd	248.2		or K Sm	996
246.5	M Gd	248.5	958	K Gd	1008
484.9	K Gd	535	1000	L Gd	1008
	or K Sm	532	1231	K Gd	1281
542.0	K Gd	592	1273	L Gd	1281
	or K Sm	589			
643.7	K Gd	694			

TABLE III. Summary of gamma-ray energies in kev as derived from electron conversion lines.

Eu^{152} $_{62}Sm_{90}^{152}$	Eu^{152} $_{64}Gd_{88}^{152}$	Eu^{154} $_{62}Sm_{92}^{154}$	Eu^{154} $_{64}Gd_{90}^{154}$
122.2	345.1		123.1
245.3	412.2		248.3
585.8	507.0		694.0
691.9	782.0		1008
969			1281
1118			
1416			
Other energies (Single conversion line, coincidence data)			
445.2			535
614	or 617		592
659	or 662		725
872	1100		759
1092			875
1170			999

similar intensities. This shows the futility of attempting a solution by using unseparated isotopes. An estimate of the contamination of Eu^{152} in the Eu^{154} is shown by observing the relative intensity of the line at 75.4 kev which is a K line for a Sm^{152} gamma ray at 122.2 kev. Similarly the conversion lines for the 345.1-kev gamma in Gd^{152} appears on the Eu^{154} photographic plates. No trace of the Eu^{154} lines was noticeable on the Eu^{152} plates. This is due to the relatively small capture cross section for neutrons in Eu^{153} compared with their capture in Eu^{151}.

The gamma rays in Gd and Sm as derived from the electron energies are listed in Table III. Certain of these are expressed with confidence where both K and L lines are observed. When only single lines are observed, the assignment to the correct daughter isotope and hence the correct energy is dependent upon coincidence observations. In a very few cases this information is not certain and alternate values are given for the gamma-ray energy.

The scintillation spectrometer was used to obtain three types of data. With the specimen of Eu^{152} near the crystal a "singles" curve showing peaks as presented in Curve A, Fig. 2, is obtained. Now by inserting the source in a cylindrical hole in the top of the crystal, a "sum" curve is obtained. This shows the additive effect of combining certain energies that are in immediate sequence such as the x-ray at 41 kev and the gamma ray at 122 kev to give a new peak at 163 kev, as shown in Curve B. Coincidence data are observed between beta energies and the complete gamma spectrum and between individual gamma peaks and the remaining gamma energies.

Those gamma transitions that are in coincidence with betas must occur in gadolinium, since no positron emission could be found from either source and K capture yields only x-ray conversion electrons. By interposing various thicknesses of aluminum between the source and detector, the approximate energy of the coincident betas was established. For example, in the Eu^{152} source the 345-kev gamma ray shows strong coincidence with beta rays of energy greater than 400 kev. The 781-kev peak is in strong coincidence with beta energies less than 400 kev and in weak coincidence with higher energy betas. Those gamma transitions

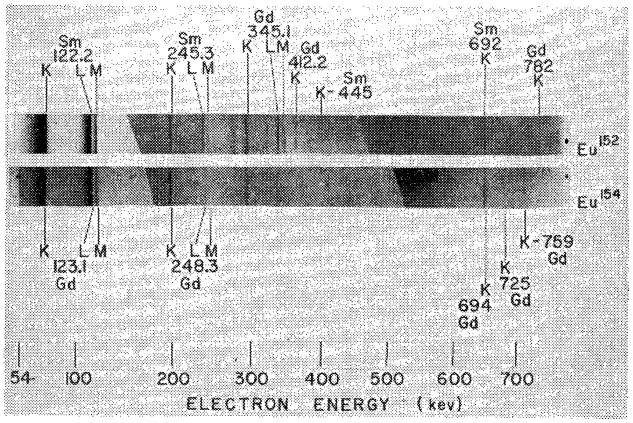

FIG. 1. Electron spectra for sources of Eu^{152} and Eu^{154} for energies from 100 to 700 kev.

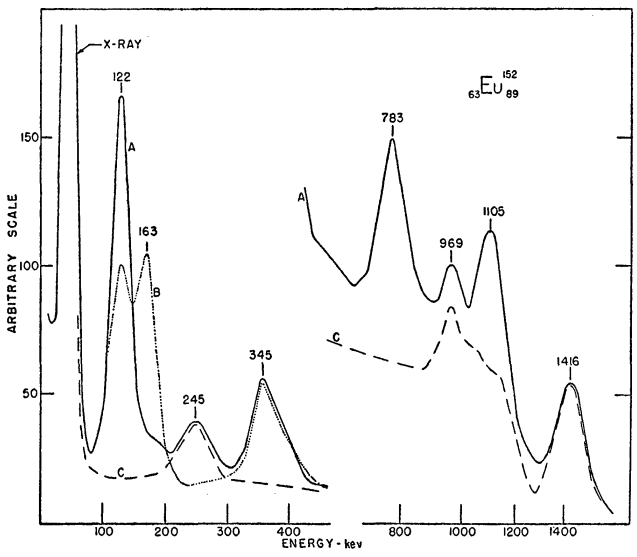

FIG. 2. Scintillation spectrometer data for Eu^{152}. (a) Singles distribution; (b) summation peaks; (c) coincidence peaks with the 122-kev gamma ray.

not in coincidence with betas are assumed to be in samarium.

Gamma-gamma coincidences are observed for each source. Curve C in Fig. 2 shows the coincidences between the 122-kev gamma ray and gamma rays of other energies. A resolution of the curves shows coincidences at 245, 872, 969, 1118, and 1416 kev. This leads to the placement of the 872-kev gamma ray in samarium even though only a single conversion line was measured for it. The 245-kev gamma ray was in coincidence with peaks at 122, 872, and 1170 kev. No coincidence could be observed between it and the 969-, 1118-, and 1416-kev gammas. The 1170-kev gamma ray was not observed by electron conversion but the coincidence peak is strong evidence that it exists. The 445- and 969-kev gamma rays were definitely in coincidence.

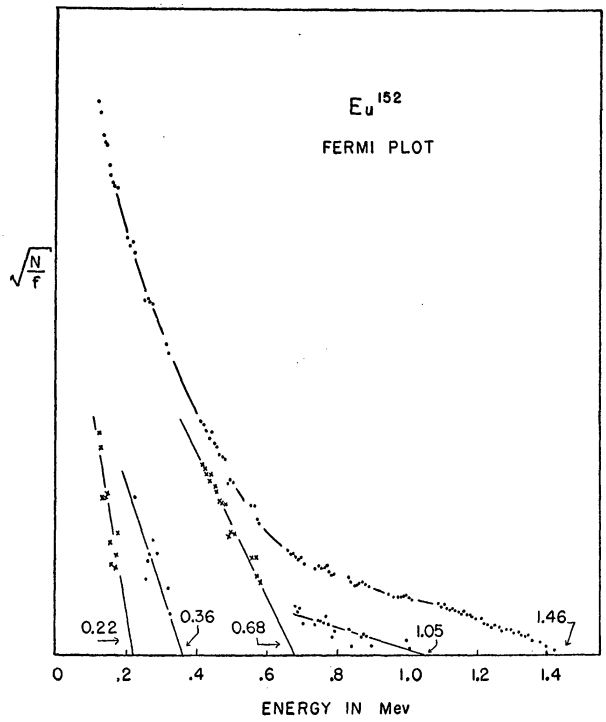

FIG. 3. Fermi plot and analysis of the beta spectrum of Eu^{152}.

In Gd^{152} the 345-kev gamma ray was found to be in coincidence with peaks at 412, 782, and 1100 kev. The 412- and 782-kev gamma rays were not in coincidence.

The entire Eu^{154} gamma spectrum was in coincidence with betas, thus indicating that all of the transitions occurred in Gd^{154} and none in Sm^{154}. The gamma ray at 123 kev was in coincidence with others at 248, 592, 694, 875, 1281, and possibly 700 and 1000 kev. The 248-kev peak was in coincidence only with energies of 123 and 759 kev. A peak in the region of 700 kev was in coincidence with another at 875 and possibly 1000 kev.

The beta spectra of Eu^{152} and Eu^{154} were observed with the double-focusing spectrometer. In each case the spectrum was found to be complex, as shown by the Fermi plots in Figs. 3 and 4. The component of highest

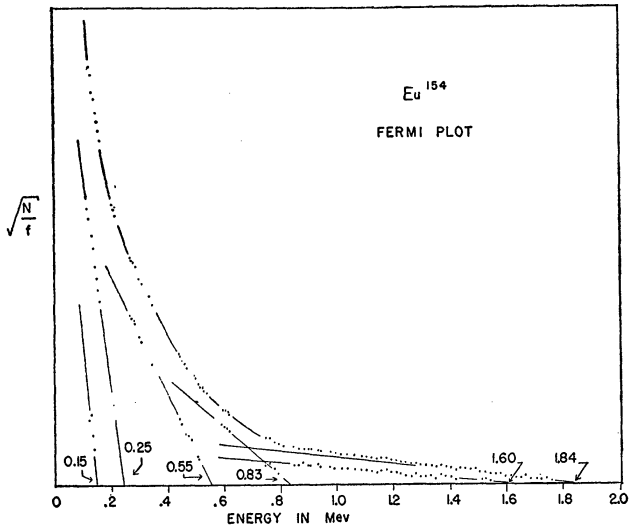

FIG. 4. Fermi plot and analysis of the beta spectrum of Eu^{154}.

energy in Eu^{152} ($E_{max}=1459$ kev) has the unique first-forbidden shape, while the 680-kev component has the allowed shape. Allowed forms are assumed for the three weaker branches. In Eu^{154} no forbidden shapes are evident. In both isotopes the successive subtraction involved in analyses of the Fermi plots lead to relatively large uncertainties in the endpoint energies of lower components. A summary of the energies, branching ratios, and logft values is presented in Table IV.

The relative intensities of a number of the internal conversion lines in both isotopes were measured, both by means of microphotometer traces of the photographic plates and with the double-focusing spectrometer. In Sm^{152} the K/L ratios for the 122- and 245-kev gamma rays are found to be 1.5 and 3.3, respectively, and that for the 345-kev gamma in Gd^{152} is 4.6, indicating that all three transitions are electric quadrupole. In Gd^{154} the 123- and 248-kev gammas have K/L ratios of 1.2 and 4.6, respectively, which are again consistent with $E2$ transitions. For the higher energy gamma rays the L lines were, in general, too weak to permit reliable intensity measurements.

The decay of Eu^{152} and Eu^{154} in every case leads to an even-even nucleus, for which the spin of the ground state is zero. The energies of the first excited states of

TABLE IV. Summary of beta transitions in Eu^{152} and Eu^{154}.

Isotope	Energy (kev)	Rel. abundance %	logft
Eu^{152}	1459±15	21	11.6
	1050±20	6	11.7
	680±20	51	10.1
	360±40	13	9.7
	220±40	9	9.1
Eu^{154}	1842±20	7	12.4
	1600±20	3	12.1
	833±30	20	10.9
	554±30	30	9.9
	246±30	28	8.9
	150±40	12	8.7

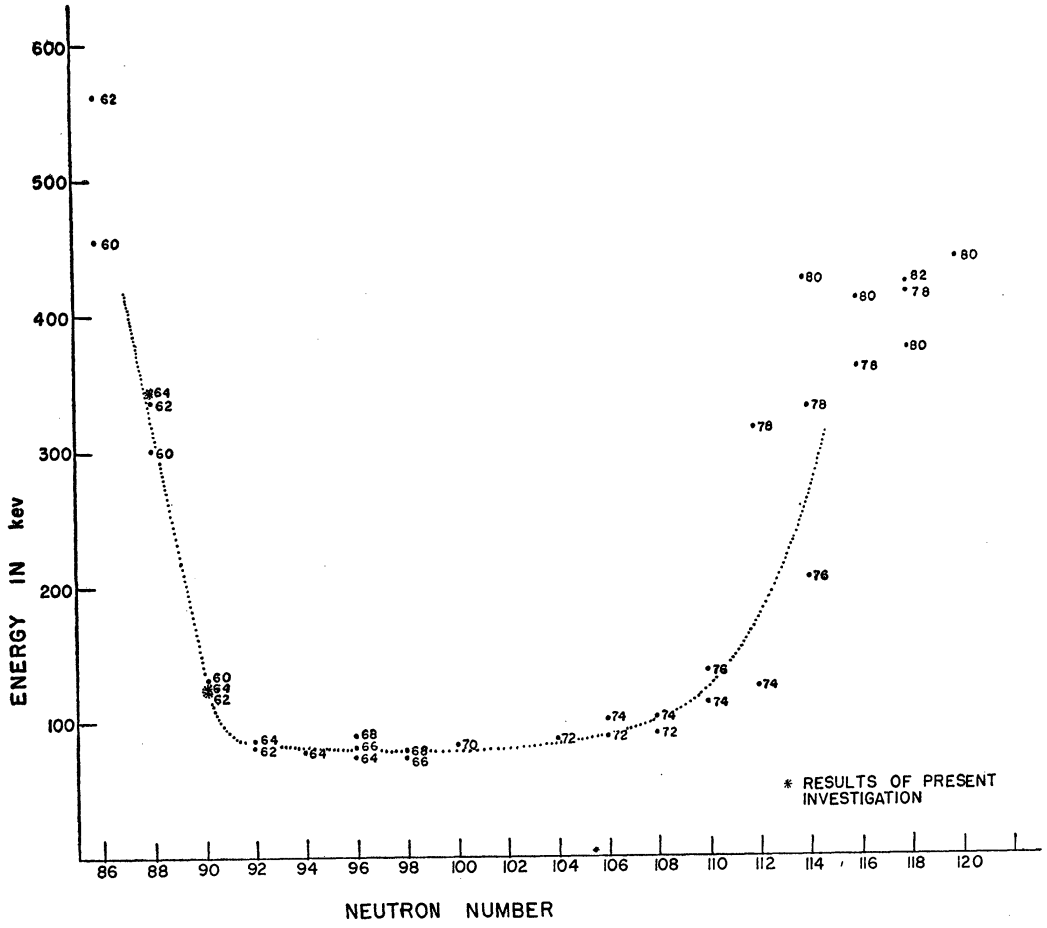

FIG. 5. The energy of first excited states for even-even nuclei as a function of neutron number.

even-even nuclei in this region depend critically upon the neutron number. The data currently available are shown in Fig. 5. The points indicated by asterisks are the results of the present investigation. The strong spectral similarity shown in Fig. 1 is really due largely to the like structures Sm^{152} and Gd^{154}, both of which have 90 neutrons.

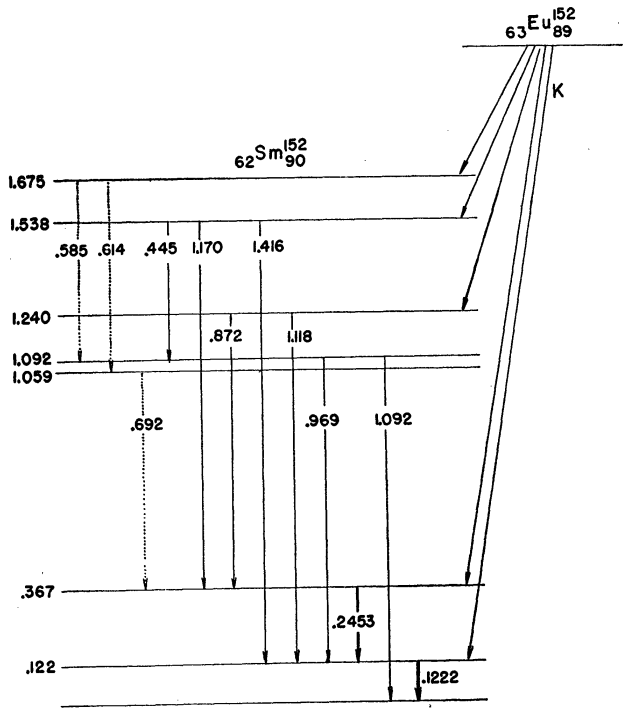

FIG. 6. Level scheme for the Sm^{152} nucleus. (Position of dotted transitions not well established.)

Level schemes for the daughter isotopes Sm^{152}, Gd^{152} and Gd^{154} are presented in Figs. 6, 7, and 8. These level schemes are consistent with the available coincidence data, and include all but three of the observed gamma transitions. The first two excited states of Sm^{152} and Gd^{154} have nearly the same energies, which is not unexpected considering that the two nuclei differ only by a pair of protons. In this region the collective model of the nucleus is expected to apply, predicting a series of rotational excited levels with even spin and parity $(0+, 2+, 4+, \cdots)$ and with energies proportional to $I(I+1)$. The expected ratio of second to first excited state energies, according to the collective model, is then 10:3, and this ratio is generally observed in the region indicated by the flat part of the curve in Fig. 5, well away from the shell closures at magic numbers.

In Sm^{152} and Gd^{154}, each with 90 neutrons, the $E2$ character of the two strong low-energy gamma rays is as expected for transitions between rotational levels, and suggests that the first and second excited states have spins 2+ and 4+, respectively. The spin assignment of 4 to the second excited state is confirmed, in the case of Gd^{154}, by the absence of a beta transition to the ground state, and the 0–2–4 spin sequence has also been established by angular correlation measurements

in both isotopes.[4] In both cases the ratio of second to first excited state energies is found to be 3:1. The small deviation from the predicted value is attributed to the fact that these isotopes lie just at the lower edge of the band of neutron numbers where the collective model is expected to hold.

In the Sm^{152} energy level scheme, K-capture branches are indicated where the estimated intensities of the gamma transitions seem to warrant them. That K-capture occurs directly to the 122-kev level is indicated by the fact that the 122-kev gamma forms a strong summation peak with the x-ray alone, as well as with other gamma rays (Curve B, Fig. 2). A comparison of the relative intensities of the 122-kev gamma ray in Sm^{152} and the 345-kev gamma ray in Gd^{152} indicates that roughly 80% of the Eu^{152} decays are by electron capture.

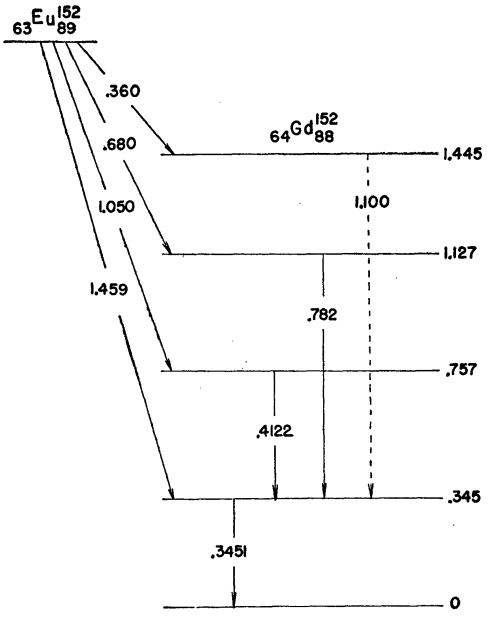

FIG. 7. Level scheme for the Gd^{152} nucleus.

In Gd^{152} no beta transition to the ground state is observed. The unique first forbidden ($\Delta I=2$, yes) shape of the highest energy transition, leading to the 345-kev excited state, suggests that the ground state spin of Eu^{152} may be 4, with odd parity. The unusually high logft values of the high-energy beta transitions are probably due to their K forbiddenness, since they go from a state with $I=K=4$ to states with $K=0$ (K being the projection of the total angular momentum on the nuclear axis of symmetry). The lowest energy beta transition ($\sim$220 kev) does not lead to an energy level from which we have observed any deexciting gamma radiation and has, therefore, not been shown in the level scheme.

[4] L. Grodzins (private communication).

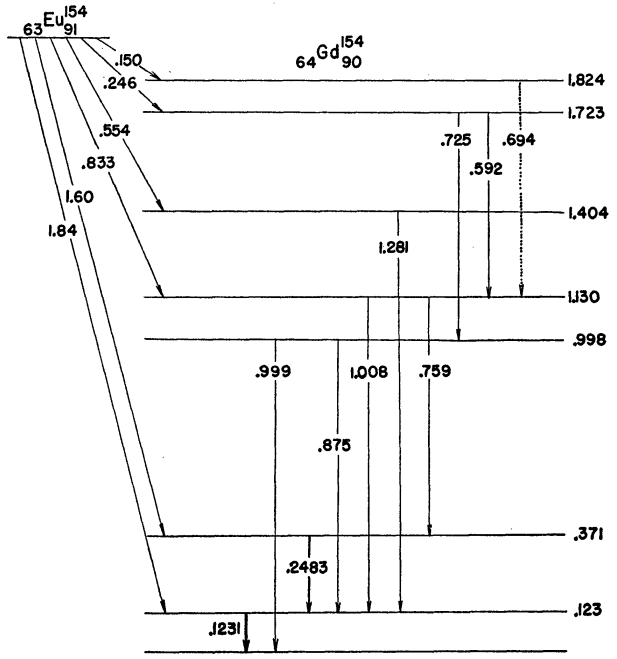

FIG. 8. Level scheme for the Gd^{154} nucleus.

No beta transition to the ground state is observed in Gd^{154}. The transitions to the first two excited levels are interpreted as ordinary first-forbidden, suggesting a spin of 3, odd parity, for the Eu^{154} ground state. The high logft values for the beta transitions are again attributed to K forbiddenness.

Coulomb excitation of Sm^{154} [5] has led to the observation of a gamma ray at 82 kev. In the present investigation no evidence for this transition appears, nor is there conclusive evidence for other transitions in Sm^{154}. Since this isotope is stable, electron capture in Eu^{154} should be energetically possible, but it may be concluded that either the branching ratio for this process is small, or most such transitions lead directly to the ground state.

The level schemes proposed here for Sm^{152} and Gd^{152} are somewhat similar to those proposed[3] by Dr. Grodzins. Certain additional gamma rays are observed while some others are not found as reported. The values of the gamma-ray energies in some cases differ, but at lower values the results from the magnetic spectrometer are undoubtedly more reliable. The level scheme proposed here for Gd^{154} is almost the same as that suggested by Stephens, again with some revision of the gamma-ray energies.

[5] N. P. Heydenburg and G. M. Temmer, Phys. Rev. **100**, 150 (1955).

II

DIRECTIONAL CORRELATION OF THE GAMMA RAYS OF Se^{76}

Reprinted from the Bulletin of the American Physical Society,
Series II, Vol. 2, No. 7, 341, November 29, 1957

Directional Correlation of the Gamma Rays of Se^{76}.*
E. G. FUNK, JR., AND M. L. WIEDENBECK, *University of Michigan.*—Directional correlation measurements have been made on the 0.65 Mev–0.55 Mev, 1.40 Mev–1.20 Mev, and 2.05 Mev–0.55 Mev gamma-ray cascades in Se^{76}. Previous investigations of the 0.65–0.55 correlation[1,2] had indicated an assignment of 2+ to the first two excited states (assuming 0+ for ground state), with a large quadrupole content (>85%) in the 2–2 transition. The present investigation of this correlation confirms these spin assignments and shows the 0.65 transition to be almost pure $E2$ (<1% Ml). The 1.40–1.20 and 2.05–0.55 correlations are consistent with a spin value of 3+ for the 2.60-Mev level, with the 1.40-Mev gamma ray being pure Ml and the 2.05-Mev transition being a mixture of 95% $E2$ and 5% Ml.

*Supported in part by the Michigan Memorial Phoenix Project and in part by the Office of Naval Research.

[1] J. J. Kraushaar and M. Goldhaber, Phys. Rev. 89, 1081 (1953).
[2] F. R. Metzger and W. B. Todd, J. Franklin Inst. 256, 277 (1953).

III

DECAY OF Gd^{161}

Reprinted from the Bulletin of the American Physical Society,
Series II, Vol. 2, No. 7, 341, November 29, 1957

Decay of Gd^{161}.* L. C. SCHMID, S. B. BURSON, *Argonne National Laboratory*, AND J. M. CORK, *University of Michigan*.— $_{64}Gd^{161}$ (3.73-min) was produced by neutron irradiation of enriched gadolinium oxide (95.4% Gd^{160}) in the Argonne reactor (CP5). This decay is characterized by β^- emission to several excited states in $_{65}Tb^{161}$. From a study of the radiations, the existence of five excited states is deduced. These have energies of 56.8, 315.5, 417.5, 481.7, and 582.8 kev. There is also evidence for a level at about 135 kev. Eleven transitions were observed. Internal-conversion-electron groups representing eight of these were measured using magnetic spectrographs. These transitions have energies of 56.8 ± 0.2, 102.0 ± 0.4, 166.2 ± 0.6, 180.8 ± 0.3, 267.3 ± 0.8, 283.9 ± 0.4, 315.5 ± 0.5, and 360.8 ± 0.5 kev. These eight, as well as transitions of 78 ± 2, 482 ± 5, and 526 ± 5 kev, were detected by scintillation methods. The transitions are fitted into a consistent decay scheme by means of coincidence measurements using the Argonne 256-channel scintillation spectrometer.

* Work performed under the auspices of the U. S. Atomic Energy Commission.

IV

DIRECTIONAL CORRELATION OF THE GAMMA RAYS OF Gd^{154}

Reprinted from the Bulletin of the American Physical Society,
Series II, Vol. 2, No. 8, 395, December 19, 1957

Directional Correlation of the Gamma Rays of Gd^{154}.* G. D. HICKMAN† AND M. L. WIEDENBECK, *University of Michigan.*—Direction correlation measurements have been made on the gamma radiation from the excited states of Gd^{154}. The results of these measurements indicate a spin sequence of $4(Q)2(Q)0$ for the 0.248 Mev -0.123 Mev correlation. Preliminary measurements on the higher excited states indicate a spin of 2 for the 0.998-Mev level, and a spin of 3 for the 1.130-Mev level. These results are in agreement with values proposed by J. O. Juliano[1] on the basis of conversion coefficients measurements. A spin of either 2 or 3 can be assigned to the 1.404 level, with a probable value of 5 for the 1.723 level. Other possible spin assignments for some of the higher excited states will be discussed.

* Supported in part by the Michigan Memorial Phoenix Project and Office of Naval Research.
† Eastman Kodak Fellow.
[1] J. O. Juliano, UCRL-3733 (1956).

V

DIRECTIONAL CORRELATION OF THE GAMMA RAYS OF Se^{76}

Accepted for publication in The Physical Review, Vol. 109

DIRECTIONAL CORRELATION OF THE GAMMA RAYS OF Se^{76}*

E. G. Funk, Jr., and M. L. Wiedenbeck
Department of Physics, University of Michigan, Ann Arbor, Michigan

(Received October 4, 1957)

Directional correlation measurements have been made on the 0.65 Mev-0.55 Mev, 2.05 Mev-0.55 Mev, and 1.40 Mev-1.20 Mev gamma-ray cascades in Se^{76} following the beta decay of 26.8-hr As^{76}. The energy levels of Se^{76} were found to have spins 0+, 2+, 2+, and 3+ in order of increasing energy. The 0.55- and 1.20-Mev gamma rays are pure electric quadrupole; the 0.65-Mev gamma ray almost pure electric quadrupole (<1% dipole); the 1.40-Mev gamma ray pure magnetic dipole; and the 2.05-Mev gamma ray a mixture of 95% electric quadrupole and 5% magnetic dipole. A possible explanation of the decay scheme in terms of vibrational levels is presented.

I. INTRODUCTION

The decay of 26.8-hr As^{76} has been investigated by many authors.[1-5] The presently accepted scheme which was proposed by Kraushaar and Goldhaber[4] and confirmed by Kurbatov, Murray and Sakai[5] is shown in Fig. 1. Directional correlation measurements have been made previously on the 0.65 Mev-0.55 Mev cascade. On the basis of results which were obtained without energy selection, Kraushaar and Goldhaber[4] assigned spin 2+ to both the 0.55-Mev and 1.20-Mev levels with the 0.65-Mev gamma ray consisting of 20-66% dipole and 80-34% quadrupole radiation. Metzger and Todd[6] repeated this correlation using pulse-height selection and confirmed the 2-2-0 assignment. Their results indicated that the 0.65-Mev gamma ray is almost pure quadrupole ($Q > 85\%$).

*Supported in part by the Michigan Memorial Phoenix Project and in part by the Office of Naval Research.

[1] K. Siegbahn, Arkiv. Mat. Astron. Fysik 34A, No. 7, 1 (1947).
[2] P. Hubert, J. phys. et radium 12, 823 (1951).
[3] P. Hubert, Ann. phys. 8, 662 (1953).
[4] J. J. Kraushaar and M. Goldhaber, Phys. Rev. 89, 1081 (1953).
[5] Kurbatov, Murray, and Sakai, Phys. Rev. 98, 674 (1955).
[6] F. R. Metzger and W. B. Todd, J. Franklin Inst. 256, 277 (1953).

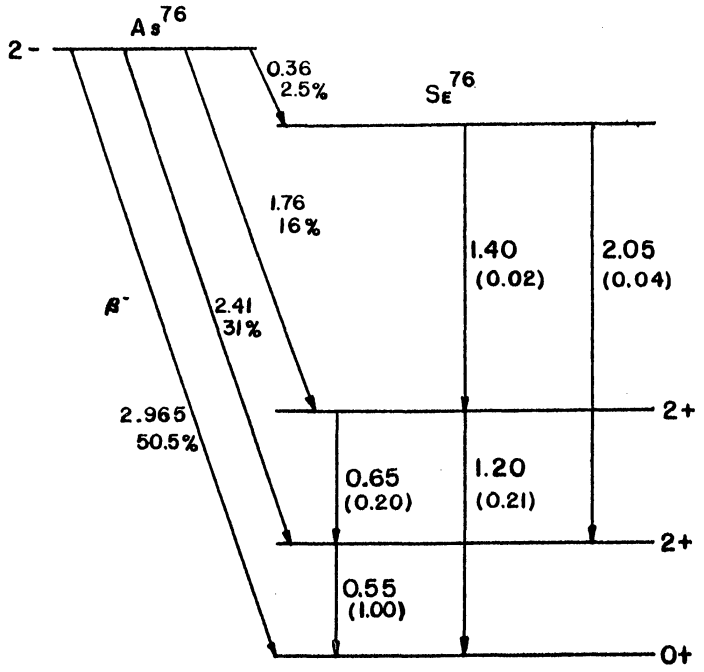

Fig. 1. Decay scheme of As^{76} proposed by Kurbatov et al.[5] (The numbers in parentheses are the relative intensities.)

Assuming the ground state of As^{76} to be 2- on the basis of Nordheim's rules[7] and considering beta-decay data and relative intensities, Kurbatov et al.[5] made a probable assignment of 3+ to the 2.60-Mev level. (The ground state spin of As^{76} has since been measured to be 2 by an atomic-beam method.[8,9]) It was decided to investigate the 2.05-0.55 and 1.40-1.20 correlations to make a definite spin assignment to the 2.60-Mev level and to reinvestigate the 0.65-0.55 correlation.

The observed gamma-ray spectrum (Fig. 2) and summing spectrum are in agreement with the decay scheme reported by Kurbatov et al.

II. EXPERIMENTAL PROCEDURE

A conventional fast-slow coincidence circuit was used for the measurements. It has an effective resolving time of 1×10^{-8} second. The instrument has been described in a previous paper.[10] The scintillation counters consisted of 2-in. x 2-in. NaI(Tl) crystals mounted on RCA type 6342 photomultipliers. The counters were shielded frontally by 3/16 in. of aluminum.

---

[7] L. Nordheim, Revs. Modern Phys. 23, 322 (1951).
[8] F. M. Pipkin and J. W. Culvahouse, Phys. Rev. 106, 1102 (1957).
[9] Christensen, Bennewitz, Hamilton, Reynolds, and Stroke, Phys. Rev. 107, 633 (1957).
[10] Stewart, Scharenberg, and Wiedenbeck, Phys. Rev. 99, 691 (1955).

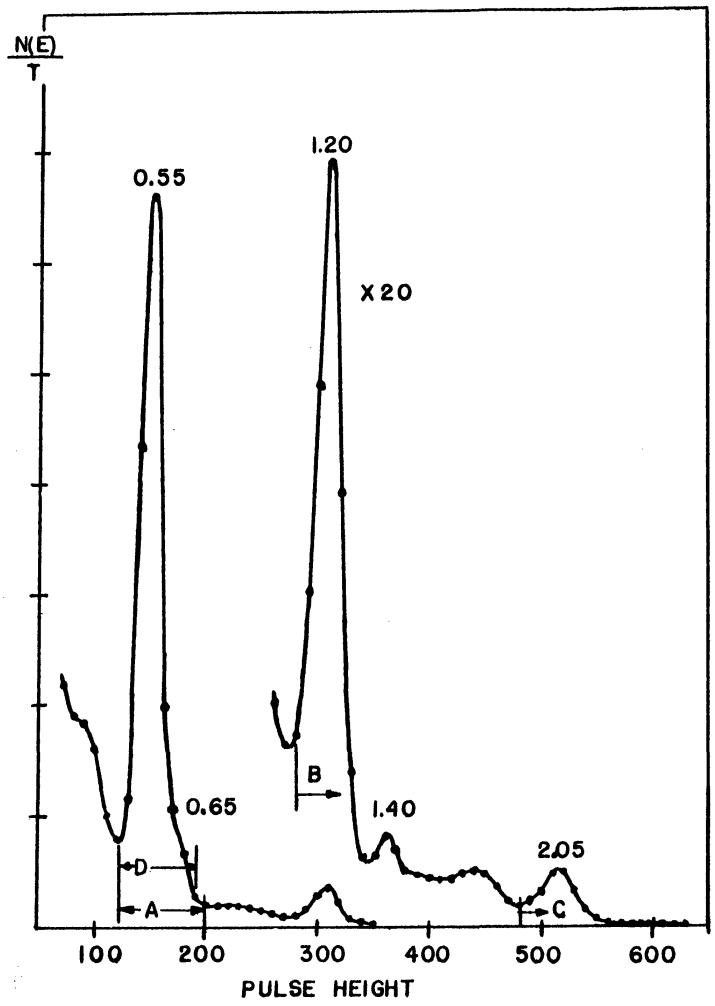

Fig. 2. Scintillation spectrum of gamma rays following the decay of As^{76}.

Although differential discrimination was used to provide energy selection, lateral lead shielding was also employed in some measurements to eliminate coincidences due to scattering.

The source material was obtained from Oak Ridge. It was in the form of As dissolved in dilute HCl. Small amounts of Sb^{122} and Sb^{124} were present in the source material. The decay was carefully studied, and it was found that the effect of the contamination on the correlations was negligible. The liquid source was contained in a cylindrically shaped Lucite holder 1/8 inch in diameter and 3/8 inch in length. All correlations were done with the source centrally mounted, a distance of 10 cm from the front face of each crystal.

The half-life of the 0.550-Mev excited state has been measured to be $(2.3 \pm 1.5) \times 10^{-11}$ sec,[11] and the half-life of the 1.20-Mev state is expected to be short. Because of this and the fact that the source was in a dilute solution, the measured correlation functions should not be attenuated due to extranuclear fields.

---

[11] C. F. Coleman, Phil. Mag. 46, 1135 (1955).

The data were taken in the sequence $90° \rightarrow (90° + \theta) \rightarrow (270° - \theta) \rightarrow 270°$, running 5 min at each angle. Measurements of the accidental coincidence rate were taken periodically. The real to accidental ratio was greater than 5 to 1 for all the correlations. The real coincidence rate was normalized by dividing by the two single counting rates N_1 and N_2 and multiplying by $N_1(180°)$ $N_2(180°)$. This method provided sufficient correction for source lifetime effects, source alignment, and any slight drift in the singles rates. A least-squares fit of the data was made to the function $W(\theta) = 1 + A_2' P_2(\cos\theta) + A_4' P_4(\cos\theta)$, where P_k is the Legendre polynomial of order k. Annihilation radiation was used to correct for the effect of finite angular resolution.[12] This correction was applied to the normalized expansion coefficients A_2' and A_4' giving the corrected coefficients A_2 and A_4.

III. RESULTS

0.65-Mev—0.55-Mev Correlation

Both differential discriminators were set at position A as shown in Fig. 2 so as to include both the 550-kev and 650-kev photopeaks. Lateral lead shielding was used for this correlation. The data are shown in Fig. 3. The solid curve is the least-squares curve corrected for finite geometry and the error flags indicate the root-mean-square statistical errors of the experimental points. The broken curve is a plot of the theoretical correlation function for a 2(Q)2(Q)0 cascade. The experimental values of the expansion coefficients corrected for finite geometry are $A_2 = -0.042 \pm 0.015$ and $A_4 = 0.319 \pm 0.023$. The errors quoted are those defined by Rose in Eq. (30).[13] If one assumes a spin of 0+ for the ground state of Se^{76} (even-even nucleus), the experimental coefficients are not compatible with any combination of spins considering pure dipole or quadrupole radiation. If a mixture in the 650-kev transition is considered, only the 2(D,Q)2(Q)0 sequence will fit the data.

The mixing parameter δ is defined as the ratio of the reduced matrix elements β and α for quadrupole and dipole radiation respectively.[14] If $\delta = \beta/\alpha$, then δ^2 is equal to the ratio of the intensities of quadrupole and dipole radiation. Q, the quadrupole content, will be equal to $\delta^2/(1+\delta^2)$, and the dipole content will be $1 - Q$. In Fig. 4 the values of A_2 and A_4 are plotted vs Q for a 2(D,Q)2(Q)0 sequence. The error flags represent the experimental values of A_2 and A_4. From Fig. 4 it is seen that the data are consistent with a value of Q equal to 0.997 ± 0.002. This is in agreement with the value of $Q > 0.85$ found by Metzger and Todd.[6]

---

[12] E. L. Church and J. J. Kraushaar, Phys. Rev. 88, 419 (1952).
[13] M. E. Rose, Phys. Rev. 91, 610 (1953).
[14] L. C. Biedenharn and M. E. Rose, Revs. Modern Phys. 25, 729 (1953).

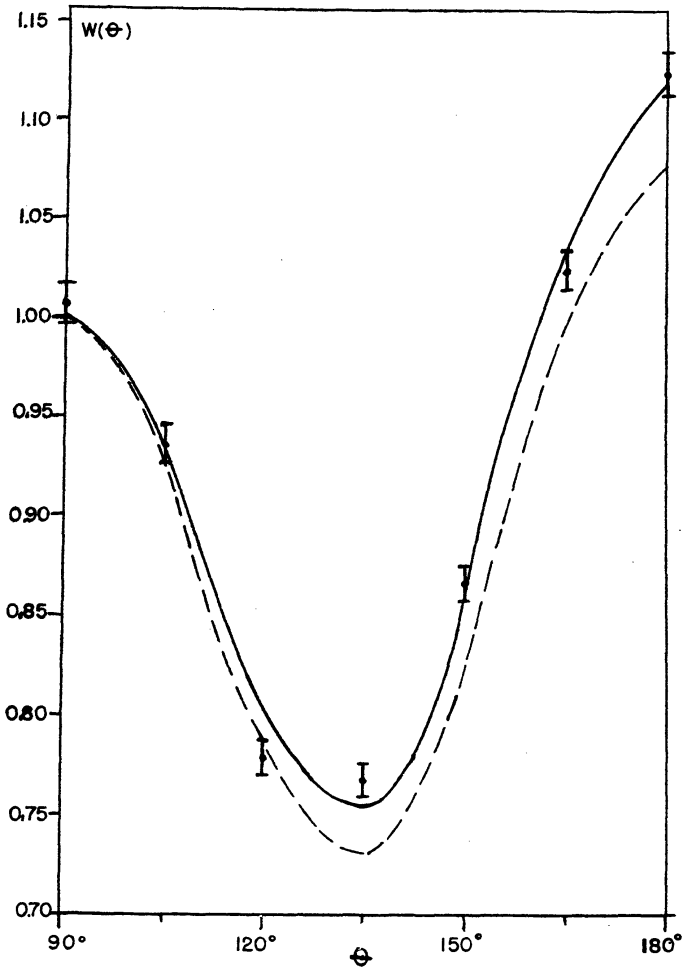

Fig. 3. Directional correlation of 0.65-0.55 Mev cascade. The solid curve is the least-squares curve corrected for finite geometry and the broken curve the theoretical correlation function for a 2(Q)2(Q)0 sequence.

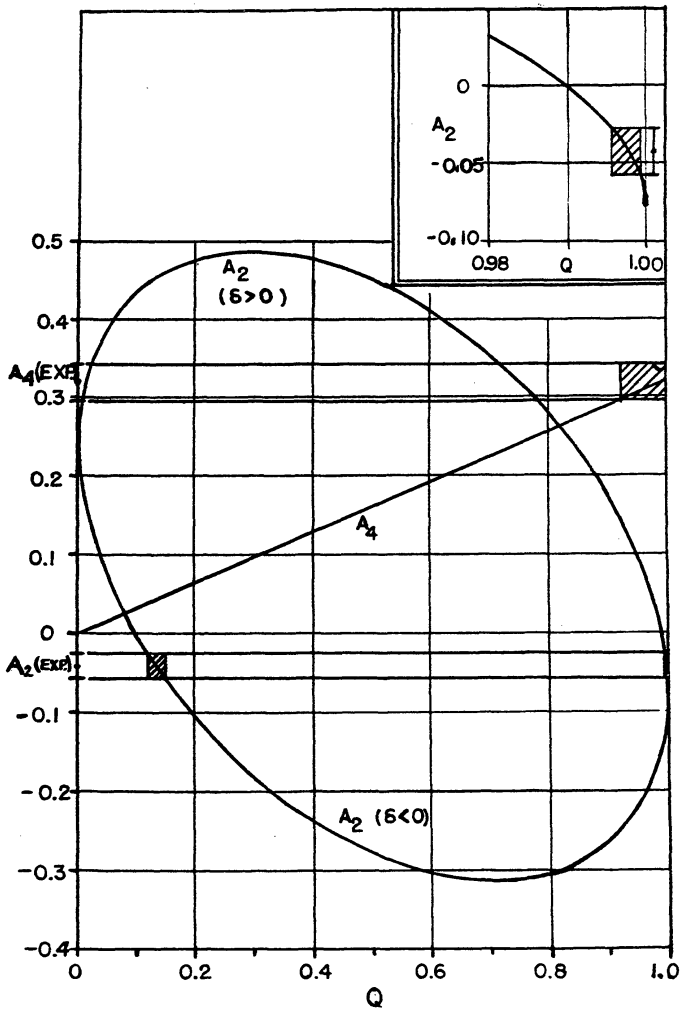

Fig. 4. A_2 and A_4 versus Q, the quadrupole intensity, for a 2(D,Q)2(Q)0 sequence. The shaded regions show the values of Q corresponding to the experimental values of A_2 and A_4.

It can thus be concluded that the first and second excited states have spins of 2_+ and that the 0.650-Mev gamma ray is a mixture of 99.7 ± 0.2% electric quadrupole and 0.3 ∓ 0.2% magnetic dipole radiation.

2.05-Mev—0.55-Mev Correlation

For the 2.05-Mev—0.55-Mev correlation, one discriminator was set integrally at C and the other differentially at D as shown in Fig. 2. Lateral lead shielding was used for this correlation. Because of the low coincidence rate, data were taken at only four angles. The experimental data and least-squares curve corrected for finite geometry are shown in Fig. 5. The corrected coefficients are $A_2 = -0.027 \pm 0.022$ and $A_4 = -0.075 + 0.033$. The negative value for A_4 rules out the combinations 4(Q)2(Q)0 and 2(D,Q)2(Q)0 since both require a positive A_4. The data can best be explained by the sequence 3(D,Q)2(Q)0. In Fig. 6 the theoretical values of A_2 and A_4 are plotted vs Q, the quadrupole content of the 3-2 transition. It is seen that the experimental values of A_2 and A_4 are compatible with a value of Q = 0.948 ± 0.014. Since an E1-M2 mixture of this magnitude is very unlikely, it is reasonable to conclude that the 2.05-Mev gamma ray consists of 94.8 ± 1.4% E2 and 5.2 ∓ 1.4% M1 radiation. On the basis of this and the selection rules for gamma transitions, a value of 3+ can be assigned to the 2.60-Mev level. This assignment agrees with that of Kurbatov *et al.*,[5] which was made on the basis of log ft values and relative intensities.

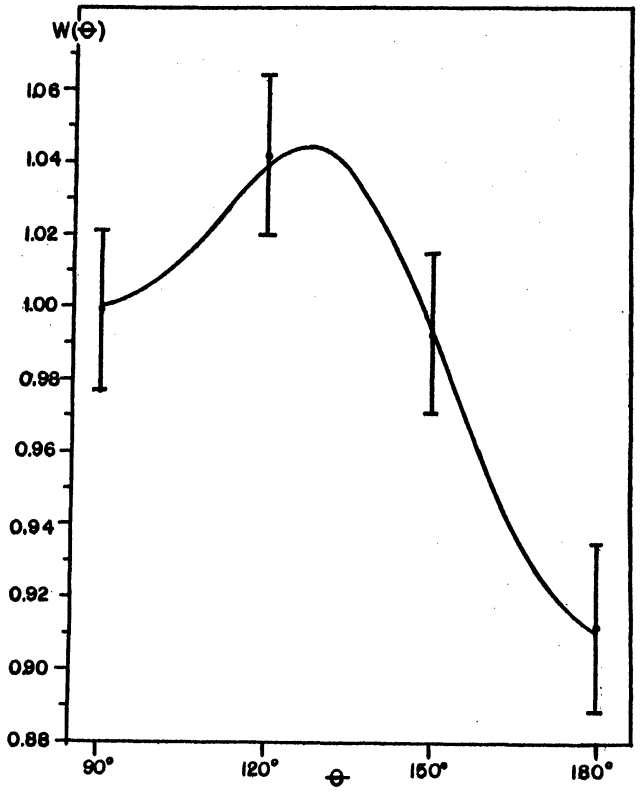

Fig. 5. Directional correlation of 2.05-Mev—0.55-Mev cascade.

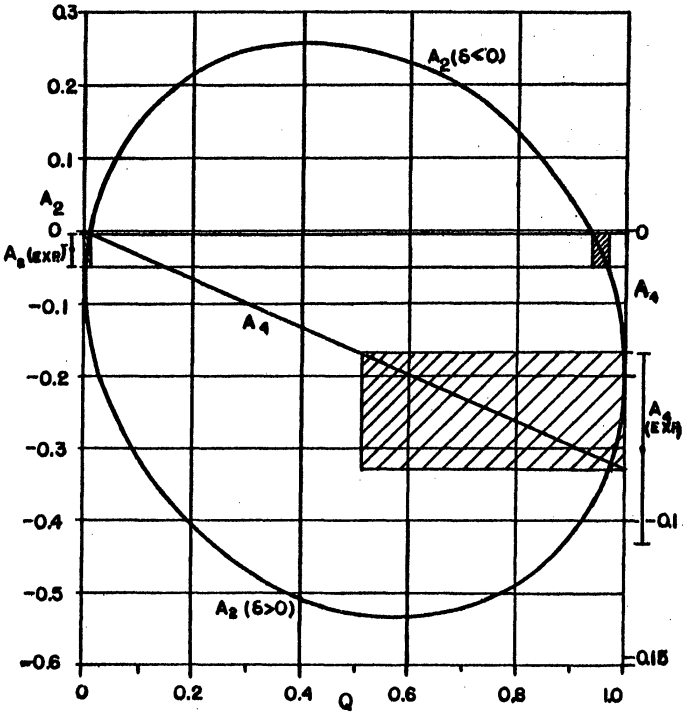

Fig. 6. A_2 and A_4 versus Q for a 3(D,Q)2(Q)0 sequence. The shaded areas indicate the values of Q corresponding to the experimental values of A_2 and A_4.

The data can almost be explained by a 1(D,Q)2(Q)0 sequence. However, a spin of 1 for the upper level is very unlikely because of the absence of the 2.60-Mev crossover transition.

1.40-Mev—1.20-Mev Correlation

For this correlation the discriminators were both set integrally at position B (Fig. 2) so as to include everything above the 1.20-Mev photopeak. No lateral lead shielding was needed. The data are shown in Fig. 7, the solid curve being the least-squares curve corrected for finite geometry and the dotted curve the theoretical curve for a 3(D)2(Q)0 combination. The corrected experimental coefficients are $A_2 = -0.076 \pm 0.022$ and $A_4 = -0.003 \pm 0.032$. It is seen that the error in A_4 is ten times larger than the coefficient itself. Thus the existence of any A_4 is questionable. When only A_2 is considered, a value of $A_2 = -0.077 \pm 0.019$ is obtained. This is in good agreement with the theoretical value of $A_2 = -0.0714$ for a 3(D)2(Q)0 cascade. Considering this sequence, the maximum amount of quadrupole admixture in the 3-2 transition consistent with the data is 0.05%. The data can also be explained by the sequence 1(D,Q)2(Q)0. However, the possibility of spin 1 for the 2.60 level has already been ruled out.

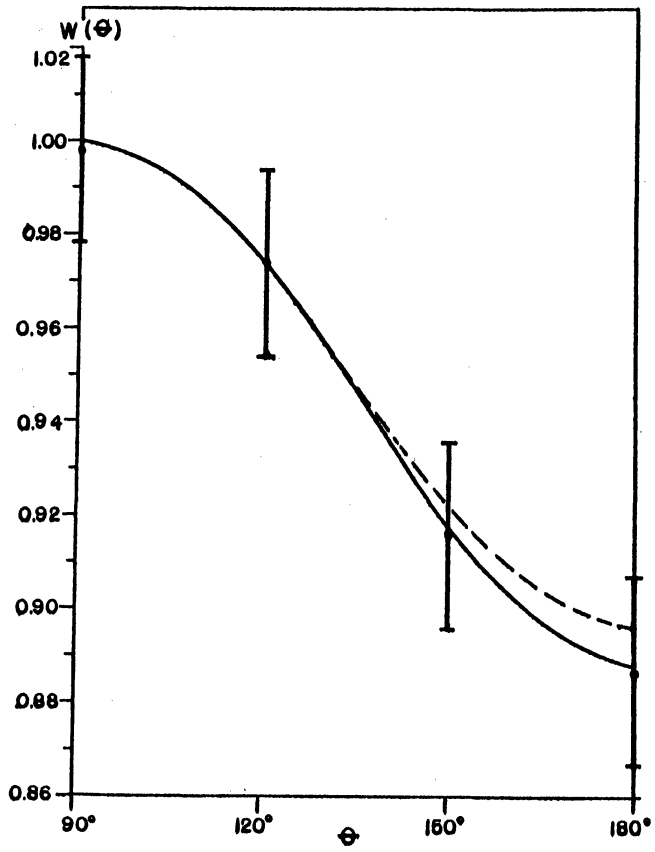

Fig. 7. Directional correlation of 1.40-Mev—1.20-Mev cascade. The solid curve is the least-squares curve corrected for finite geometry and the broken curve the theoretical correlation function for a 3(D)2(Q)0 combination.

Thus a spin of 3+ can be assigned to the 2.60-Mev level with the 1.40-Mev gamma ray being almost pure M1.

IV. SUMMARY AND DISCUSSION

The results of the correlations confirm the assignment of 0+, 2+, 2+, 3+ to the energy levels of Se^{76} in order of increasing energy. The 0.55-Mev and 1.20-Mev gamma rays are found to be pure E2 radiation, the 0.65-Mev gamma ray 99.7 ± 0.2% E2 and 0.3 ∓ 0.2% M1, the 2.05-Mev gamma ray 94.8 ± 1.4% E2 and 5.2 ∓ 1.4% M1, and the 1.40-Mev gamma ray almost pure M1.

In the intermediate regions between closed-shell nuclei and those nuclei with many particles in unfilled shells, excited states corresponding to quadrupole vibrations about a spherical equilibrium shape are expected. An enhancement of E2 transition probabilities is usually associated with these vibrational states. A review of the theory of vibrational excitations and a summary of experimental data on nuclei in these regions has been presented in the review article on Coulomb excitation by Alder et al.[15]

Se^{76} is one of the nuclei which exhibits vibrational states. The first excited state in Se^{76} has been reached by Coulomb excitation, and the cross section for this process was found to be much larger than the cross section expected for a single-particle excitation.[16] This is strong evidence that the excitation is due mainly to a cooperative vibrational motion involving many nucleons. Thus the first excited state is mainly the result of a one-phonon vibrational excitation.

The ratio of the energies of the second and first excited states and the fact that the 0.65-Mev gamma ray is almost pure E2 indicate that the second excited state is also mainly vibrational in character, probably a two-phonon vibrational excitation. If there were no coupling between the vibrational motion and the individual particle motion of the outer nucleons, the two-phonon vibrational state would be three-fold degenerate with spins 0, 2, 4 and even parity. However, this coupling, which can be very complex, usually splits the three levels. The very different nature of the two transitions originating from the third excited state is difficult to understand. One possibility is that the third excited state is due to a two-phonon vibrational excitation coupled with a single-particle excitation of the ground state configuration. If this is true, then the 1.40-Mev gamma ray occurs between two states with the same number of phonons and is primarily a single-particle transition. This could account for the fact

---

[15] Alder, Bohr, Huus, Mottelson, and Winther, Revs. Modern Phys. 28, 432 (1956).

[16] G. M. Temmer and N. P. Heydenburg, Phys. Rev. 104, 967 (1956).

that the 1.40-Mev gamma ray is almost pure dipole radiation. However, the 2.05-Mev transition would require both a change in phonon number and particle excitation. This could give an enhanced E2 transition probability and might account for the large E2 component in the 2.05-Mev transition.

ACKNOWLEDGMENTS

The authors wish to acknowledge the help of F. C. Chang and R. Arns in recording some of the data.

VI

A RE-EVALUATION OF THE BETA AND GAMMA ENERGIES FROM Ho^{166}, Nd^{147}, AND Sm^{153}

Reprinted from the Bulletin of the American Physical Society,
Series II, Vol. 3, No. 1, 64, January 29, 1958

A Re-Evaluation of the Beta and Gamma Energies from Ho^{166}, Nd^{147}, and Sm^{153}. J. M. CORK, M. K. BRICE, R. G. HELMER, AND R. M. WOODS, JR., *University of Michigan.**— Using enriched sources of Ho^{165}, Nd^{146}, and Sm^{152} strong specimens of Ho^{166}, Nd^{147}, and Sm^{153} were made by neutron capture. Studies of the strong sources by both magnetic and scintillation spectrometers showed the existence of some gamma rays not previously reported, more exact values for the low-energy gamma rays, and better resolution of the components of the beta spectra. In Ho^{166} gamma rays occur at 80.25, 970, 1377, 1540, and 1620 kev, and the maximum beta energies are 1839, 1758, 869, 380, and 220 kev. Nd^{147} yields gamma rays at 91.3, 120.6, 198.2, 277.0, 321, 400, 441, 533, 597, and 688 kev, with beta components at 812, 380, and 230 kev. In Sm^{153} gamma rays are found at 69.8, 103.5, and 173.6 kev and beta components at 813, 710, and 640 kev. A level scheme is presented for each nucleus that is in complete agreement with observed data.

VII

INTERPRETATION OF GAMMA-GAMMA DIRECTIONAL CORRELATIONS INVOLVING DIPOLE-QUADRUPOLE MIXTURES

INTERPRETATION OF GAMMA-GAMMA DIRECTIONAL CORRELATIONS INVOLVING DIPOLE-QUADRUPOLE MIXTURES*

R. G. Arns** and M. L. Wiedenbeck
Department of Physics, University of Michigan, Ann Arbor, Michigan

A collection of curves is presented which is intended to provide a quick method for interpreting γ-γ directional correlations when one or both gamma rays involve a mixture of dipole and quadrupole radiation. The present work is based on the previous calculation of F-coefficients by Ferentz and Rosenzweig.[1] The range of spins included is expected to cover most cases of practical interest.

I. TRANSITIONS OF MIXED MULTIPOLARITY IN γ-γ CORRELATION

Denote j_1, j, and j_2 as the initial, intermediate, and final momenta of a cascade in the gamma decay of a nucleus. Let the transition between j_1 and j be a mixture of 2^{L_1} and 2^{L_1+1} poles. Similarly describe the second transition as a mixture of 2^{L_2} and 2^{L_2+1} poles. The theoretical angular correlation function will then be of the form:

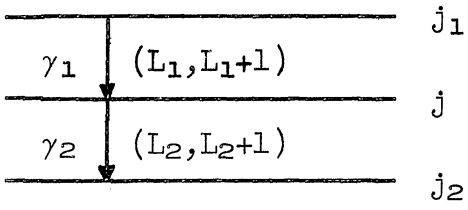

$$W(\Theta) = \sum_{K \text{ even}} A_K^{(1)'} A_K^{(2)'} P_K (\cos \Theta) \qquad (1)$$

in which the constant $A_K^{(\nu)'}$ for the νth transition is dependent only upon the spins and multipolarities involved in that transition. The $A_K^{(\nu)'}$ are of the form:

---

*Supported in part by the Michigan Memorial Phoenix Project and by the Office of Naval Research.

**Dow Chemical Company Fellow.

[1] M. Ferentz and N. Rosenzweig, ANL-5324 (1955).

$$A_K^{(\nu)'} = F_K(L_\nu,L_\nu,j_\nu,j) + 2\delta_\nu F_K(L_\nu,L_\nu+1,j_\nu,j) + \delta_\nu^2 F_K(L_\nu+1,L_\nu+1,j_\nu,j) \tag{2}$$

The summation over K in (1) runs from zero to the least of 2j, $2(L_1+1)$, or $2(L_2+1)$. The $F_K(L,L',j',j)$ are the F-coefficients as defined and tabulated by Ferentz and Rosenzweig.[1] δ_ν^2 is the ratio of the intensity of the $L_\nu + 1$ radiation to the L_ν radiation in the νth transition of the cascade.

The least-squares fit of experimental points in an angular correlation experiment[2] is normally made to the function:

$$W(\Theta) = 1 + G_2A_2P_2(\cos\Theta) + G_4A_4P_4(\cos\Theta) \tag{3}$$

where the G_K are attenuation factors dependent upon the geometry of the experiment, etc., and:

$$A_K = \left(\frac{A_K^{(1)'}}{A_o^{(1)'}}\right)\left(\frac{A_K^{(2)'}}{A_o^{(2)'}}\right) . \tag{4}$$

Due to the special properties of the F-coefficient, viz:

$$F_o\,(L,L,j',j) = 1 \tag{5}$$

$$F_o\,(L,L+1,j',j) = 0 , \tag{6}$$

equation (4) becomes:

$$A_K = A_K^{(1)}\,A_K^{(2)} = \left(\frac{A_K^{(1)'}}{1+\delta_1^2}\right)\left(\frac{A_K^{(2)'}}{1+\delta_2^2}\right) \tag{7}$$

Define Q_ν as the fraction of the $L_\nu + 1$ multipole in the νth (mixed) transition. Q_ν bears the following relation to δ_ν:

$$Q_\nu = \frac{\delta_\nu^2}{1+\delta_\nu^2} . \tag{8}$$

Then $1 - Q_\nu$ is the fraction of the L_ν multipole in the same transition and, upon substitution, equation (7) becomes:

---

[2] M. E. Rose, Phys. Rev. 91, 610 (1953).

$$A_K = A_K^{(1)}\, A_K^{(2)} = [F_K(L_1,L_1,j_1,j)(1-Q_1) + 2F_K(L_1,L_1+1,j_1,j)\sqrt{Q_1(1-Q_1)} +$$

$$F_K(L_1+1,L_1+1,j_1,j)Q_1]\,[F_K(L_2,L_2,j_2,j)(1-Q_2) +$$

$$2F_K(L_2,L_2+1,j_2,j)\sqrt{Q_2(1-Q_2)} + F_K(L_2+1,L_2+1,j_2,j)Q_2] \quad . \qquad (9)$$

II APPLICATION TO CASCADES WITH MIXTURE IN ONE TRANSITION

Equation (9) takes on an especially simple form when one transition is a mixture of dipole and quadrupole radiation and the other is unmixed. If, for example, the mixture is in the first transition:

$$A_2 = A_2^{(1)}\, A_2^{(2)} = [a(1-Q) + b\sqrt{Q(1-Q)} + cQ]\, F_2(L_2,L_2,j_2,j) \qquad (10)$$

$$A_4 = A_4^{(1)}\, A_4^{(2)} = [dQ]\, F_4(L_2,L_2,j_2,j) \qquad (11)$$

where: $a = F_2(1,1,j_1,j)$

$b = 2F_2(1,2,j_1,j)$

$c = F_2(2,2,j_1,j)$

$d = F_4(2,2,j_1,j)$. (12)

In terms of the first transition only:

$$A_2^{(1)} = [a(1-Q) + b\sqrt{Q(1-Q)} + cQ] \qquad (13)$$

$$A_4^{(1)} = dQ \quad . \qquad (14)$$

A plot of $A_2^{(1)}$ vs Q for equation (13) is an ellipse. Equation (14) is a straight line in the variables $A_4^{(1)}$ and Q. The curves tabulated in this report are plots of $A_2^{(\nu)}$ vs Q and $A_4^{(\nu)}$ vs Q for single transitions between states of various spins.

The least-squares fit will yield values of $A_2^{(EXP)} \pm \epsilon_2$ and $A_4^{(EXP)} \pm \epsilon_4$ where the ϵ_K are the R.M.S. statistical errors. In order to determine the quadrupole content of the mixed transition, the $A_2^{(EXP)} \pm \epsilon_2$ and $A_4^{(EXP)} \pm \epsilon_4$ must be divided by the corresponding F-coefficients from the unmixed transition [cf. equations (10) and (11)]. The resultant numbers are then compared with the graph in order to find the range of Q consistent with the experiment.

$A_2^{(\nu)}$ and $A_4^{(\nu)}$ are plotted to the same scale vs Q in the following graphs. The absence of an $A_4^{(\nu)}$ line indicates $A_4^{(\nu)} = 0$.

III. APPLICATION TO CASCADES WITH MIXTURES IN BOTH TRANSITIONS

If both steps of a cascade are mixtures of dipole and quadrupole radiation, equation (9) assumes the form:

$$A_2 = A_2^{(1)} A_2^{(2)} = [a_1(1-Q_1) + b_1\sqrt{Q_1(1-Q_1)} + c_1Q_1][a_2(1-Q_2) + b_2\sqrt{Q_2(1-Q_2)} + c_2Q_2] \quad (15)$$

$$A_4 = A_4^{(1)} A_4^{(2)} = [d_1Q_1][d_2Q_2] \quad (16)$$

where a_1, a_2, etc., are defined as in (12) and Q_1 and Q_2 are again to be found by graphical analysis. In this case a value of $A_K^{(\nu)}$ cannot be assumed for either transition. However, the set of values of $A_K^{(\nu)}$ satisfying:

$$A_2^{(1)} A_2^{(2)} = A_2^{(EXP)} \pm \epsilon_2 \quad (17)$$

$$A_4^{(1)} A_4^{(2)} = A_4^{(EXP)} \pm \epsilon_4 \quad (18)$$

can be calculated. The values of $A_2^{(1)}$ and $A_2^{(2)}$ satisfying (17) can be plotted against one another to the same scale as the single transition mixture curves of this report. (Any graph paper with 20 lines to the inch will suffice.) Various single transition mixture curves can be placed with scales to coincide with the $A_K^{(\nu)}$ axes of the experimental graph [i.e., graph of equation (17)]. Then a value of Q_1 consistent with the first transition will correspond to a range of values of Q_2 for the second transition required by the experimental graph and vice versa. The same procedure can also be applied to equation (18).

IV. NOTATION

Each curve is identified by the spins of the two states involved in the transition. They are listed in the form: j(D,Q)j', where in all cases j is the spin of the intermediate state. j' is the spin of the initial or

final state of the cascade depending on whether the graph is used to describe the first or second transition.

A list of the coefficients a, b, c, and d used in computing the graphs is appended in Table I.

Often it is desirable to know the mixing in terms of δ, the mixing parameter. In each case where b [as defined in (14) and listed in Table I] is positive, the upper portion of the ellipse corresponds to δ positive. If b is negative, the opposite is true.

TABLE I. COEFFICIENTS a, b, c, AND d USED IN COMPUTATION OF THE SINGLE TRANSITION MIXTURE CURVES

j	j'	a	b	c	d
1	1	-0.3536	-2.1213	-0.3536	0
1	3	+0.0707	+0.9487	+0.3536	0
2	1	+0.4183	-1.8708	-0.2988	+0.7127
2	2	-0.4183	-1.2247	+0.1281	-0.3054
2	3	+0.1195	+1.3093	+0.3415	+0.0764
3	2	+0.3464	-1.8974	-0.1237	+0.6701
3	3	-0.4330	-0.8660	+0.2268	-0.4467
3	4	+0.1443	+1.4434	+0.3093	+0.1489
4	3	+0.3134	-1.8804	-0.0448	+0.6088
4	4	-0.4388	-0.6708	+0.2646	-0.4981
4	5	+0.1595	+1.5136	+0.2849	+0.1937
5	4	+0.2944	-1.8619	0.0000	+0.5666
5	5	-0.4416	-0.5477	+0.2831	-0.5230
5	6	+0.1698	+1.5566	+0.2669	+0.2241
6	5	+0.2820	-1.8464	+0.0288	+0.5370
6	6	-0.4432	-0.4629	+0.2936	-0.5370
3/2	1/2	+0.5000	-1.7321	-0.5000	0
3/2	3/2	-0.4000	-1.5492	0.0000	0
3/2	5/2	+0.1000	+1.1832	+0.3571	0
5/2	3/2	+0.3742	-1.8974	-0.1909	+0.7054
5/2	5/2	-0.4276	-1.0142	+0.1909	-0.3968
5/2	7/2	+0.1336	+1.3887	+0.3245	+0.1176
7/2	5/2	+0.3273	-1.8898	-0.0779	+0.6367
7/2	7/2	-0.4364	-0.7559	+0.2494	-0.4775
7/2	9/2	+0.1528	+1.4832	+0.2962	+0.1737
9/2	7/2	+0.3028	-1.8708	-0.0197	+0.5857
9/2	9/2	-0.4404	-0.6030	+0.2752	-0.5125
9/2	11/2	+0.1651	+1.5374	+0.2752	+0.2102

1 (D,Q) 1

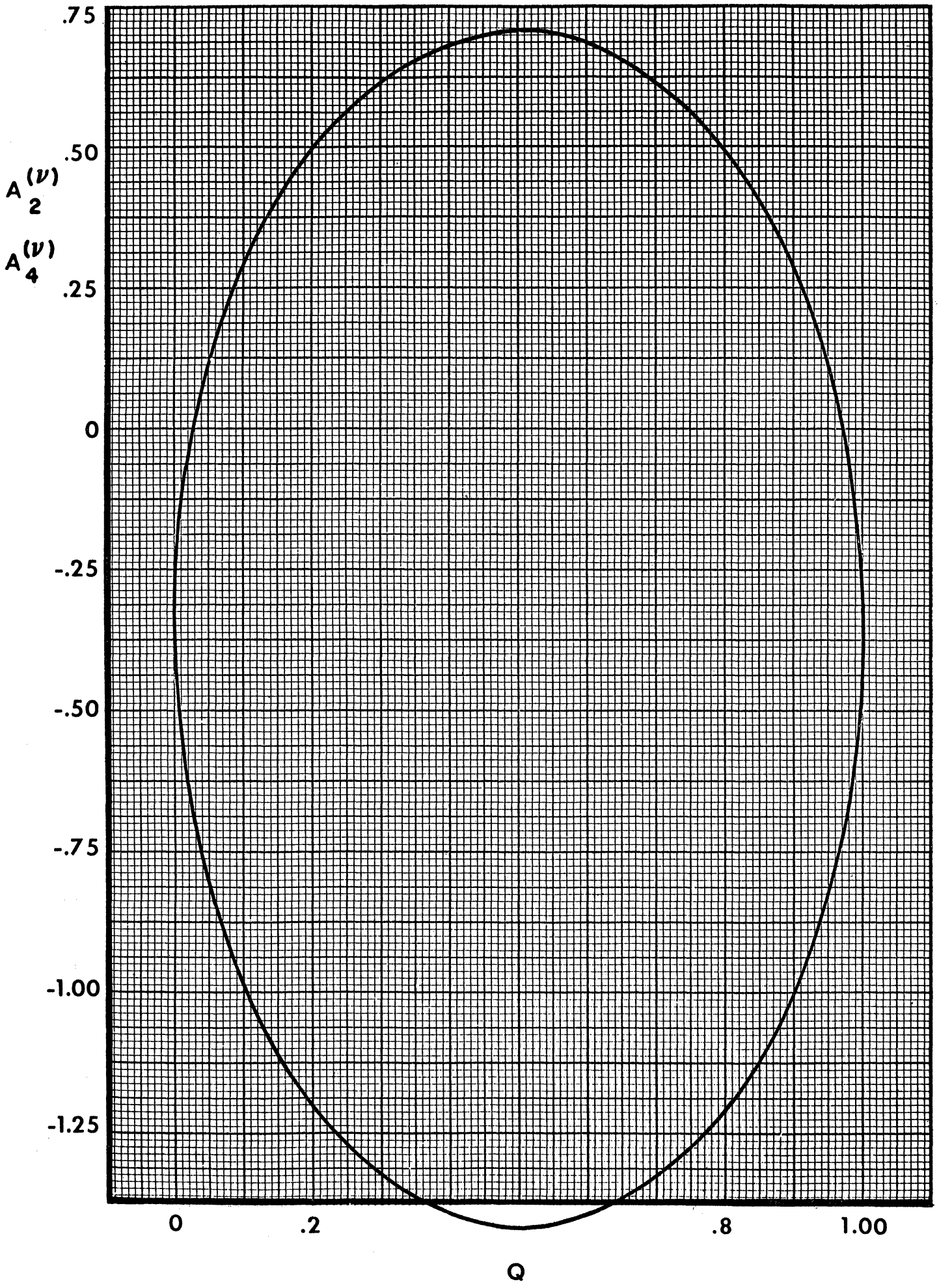

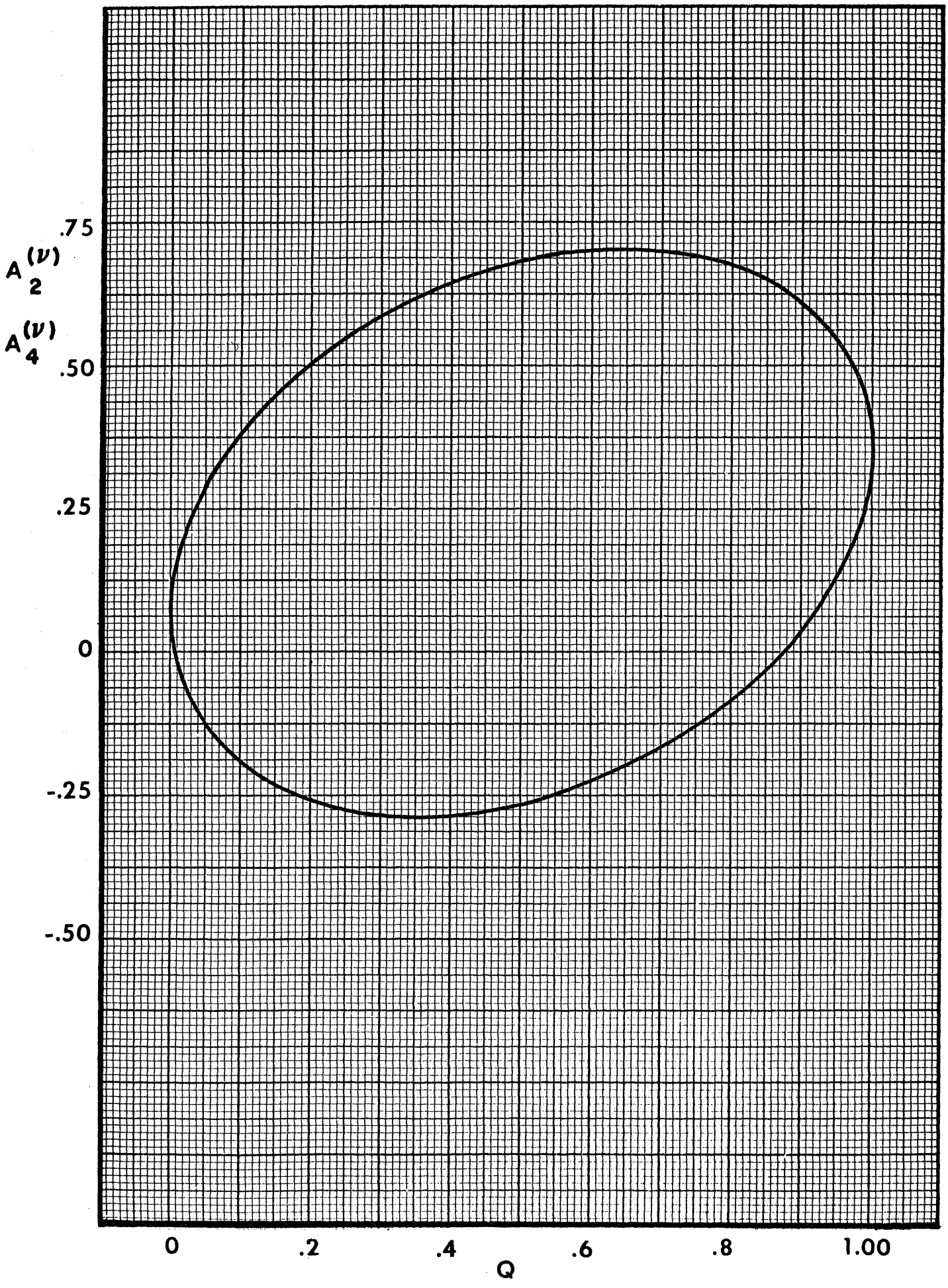
1 (D,Q) 2
J = 1, J' = 2
.75
$A_2^{(\nu)}$
$A_4^{(\nu)}$
.50
.25
0
-.25
-.50
0
.2
.4
.6
.8
1.00
Q

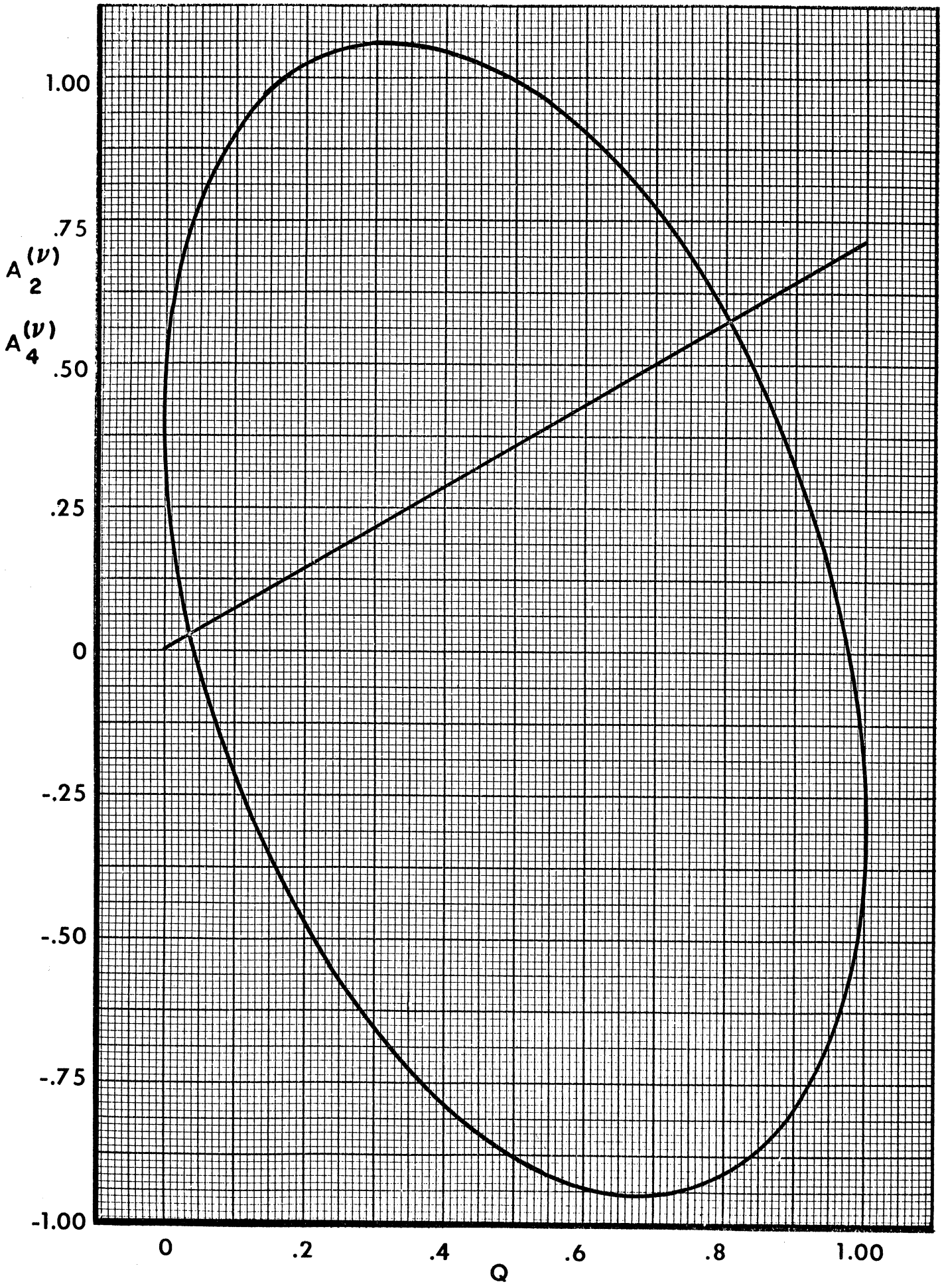
2 (D,Q) 1
J=2, J'=1
1.00
.75
$A_2^{(\nu)}$
$A_4^{(\nu)}$
.50
.25
0
-.25
-.50
-.75
-1.00
0
.2
.4
.6
.8
1.00
Q

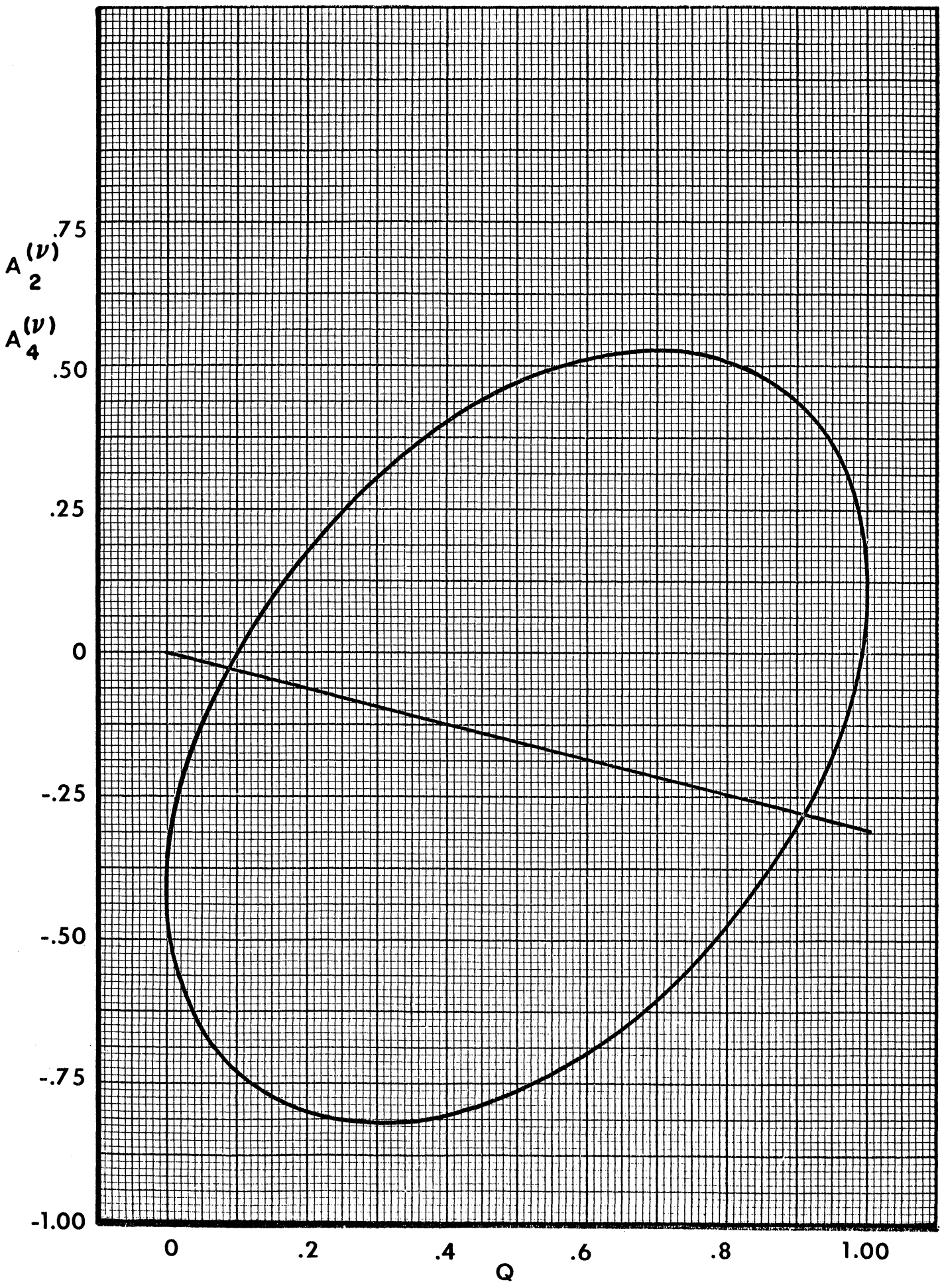
2 (D,Q) 2
.75
$A_2^{(\nu)}$
$A_4^{(\nu)}$
.50
.25
0
-.25
-.50
-.75
-1.00
0
.2
.4
.6
.8
1.00
Q

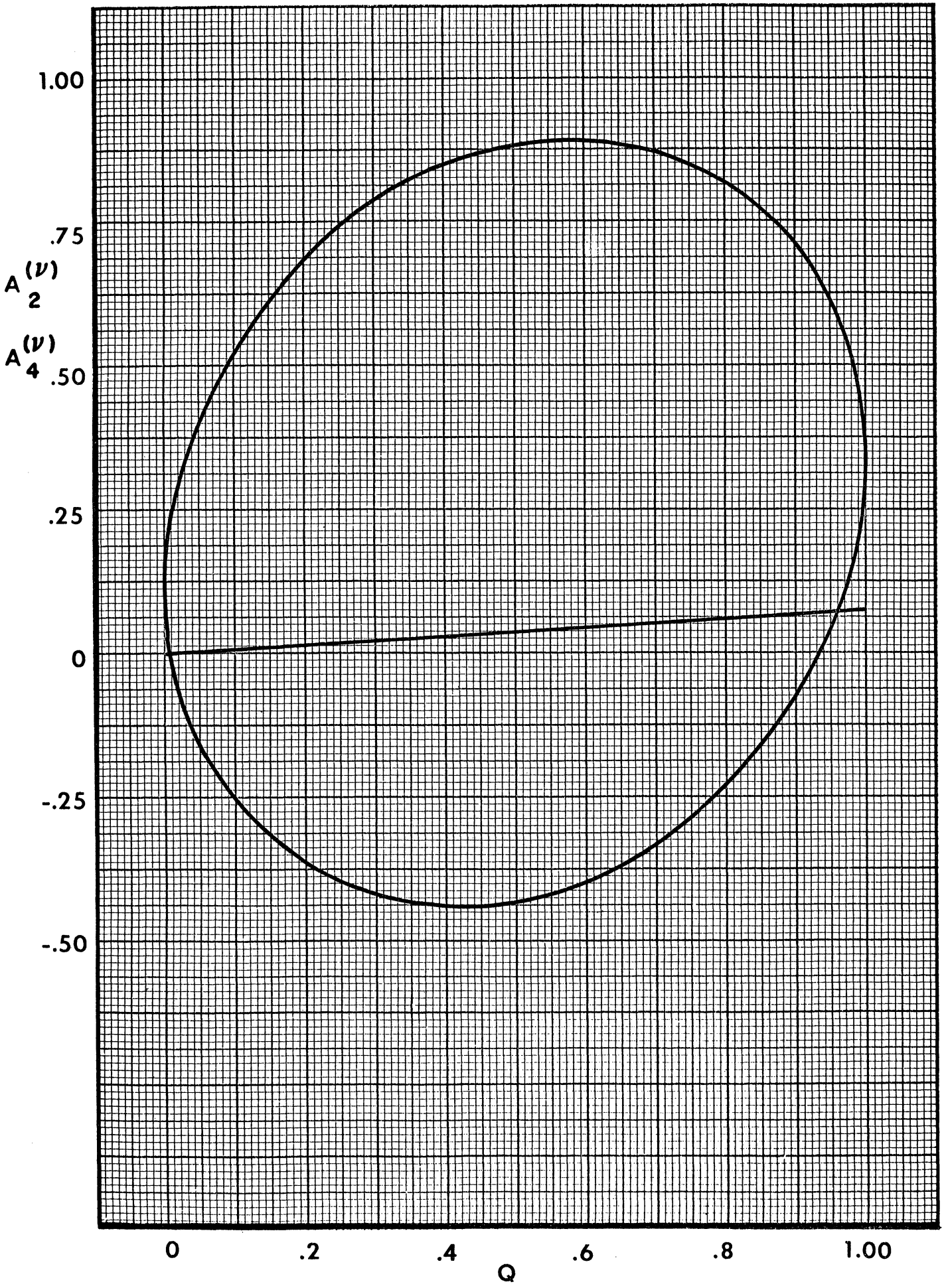
2 (D,Q) 3
J = 2, J' = 3
1.00
.75
$A_2^{(\nu)}$
$A_4^{(\nu)}$
.50
.25
0
-.25
-.50
0
.2
.4
.6
.8
1.00
Q

3 (D,Q) 2
J = 3, J' = 2

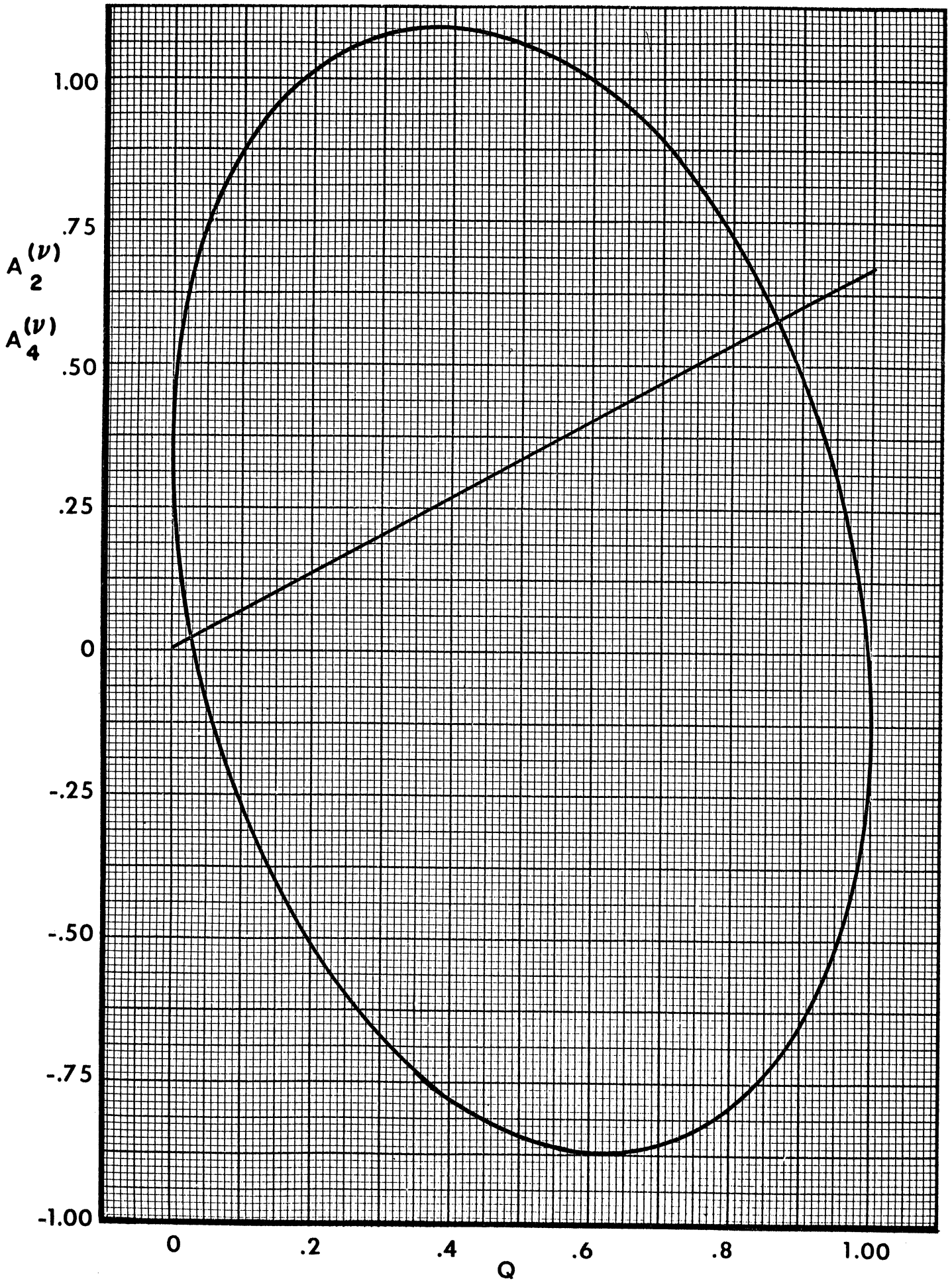

3 (D,Q) 3

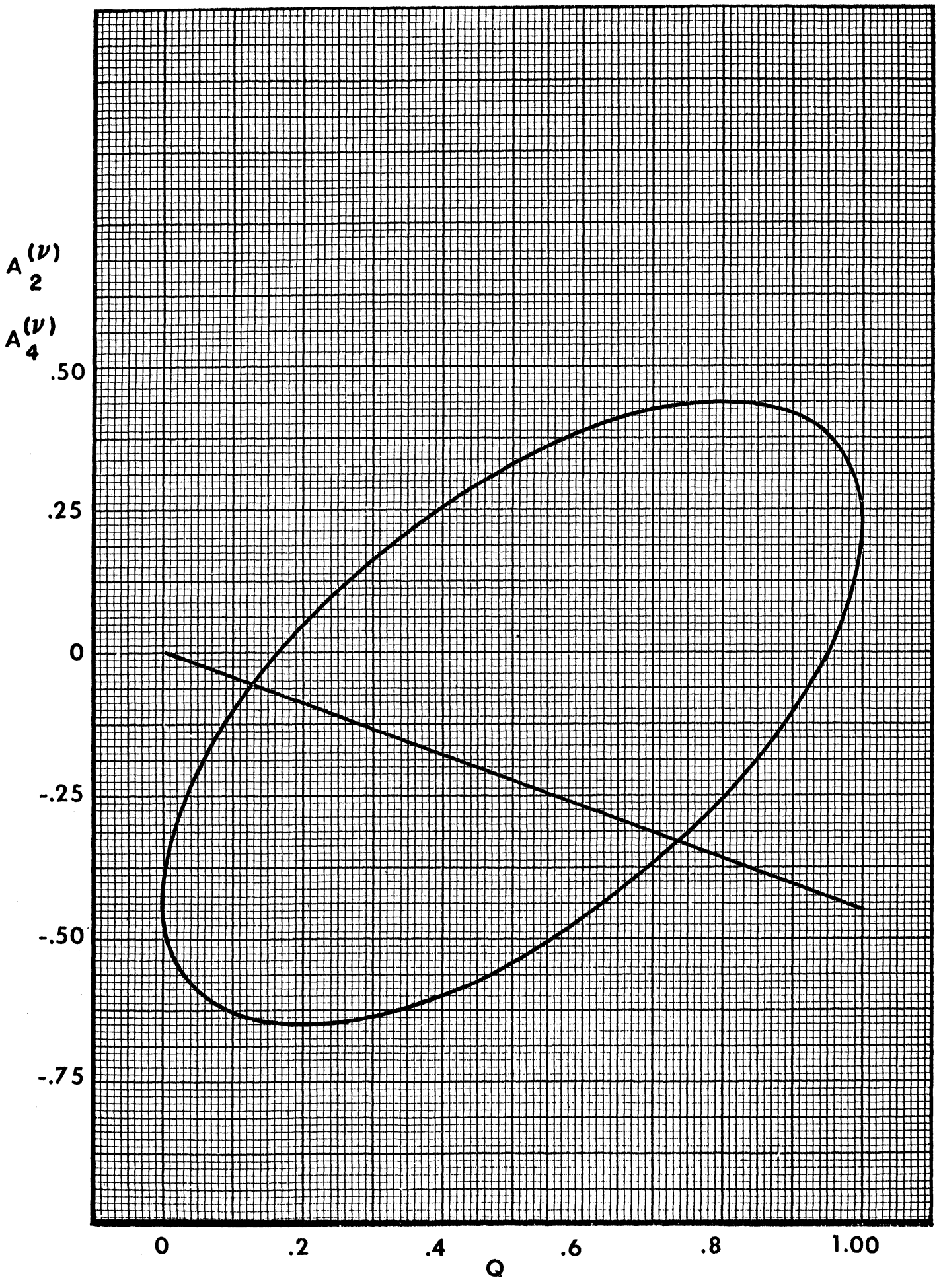

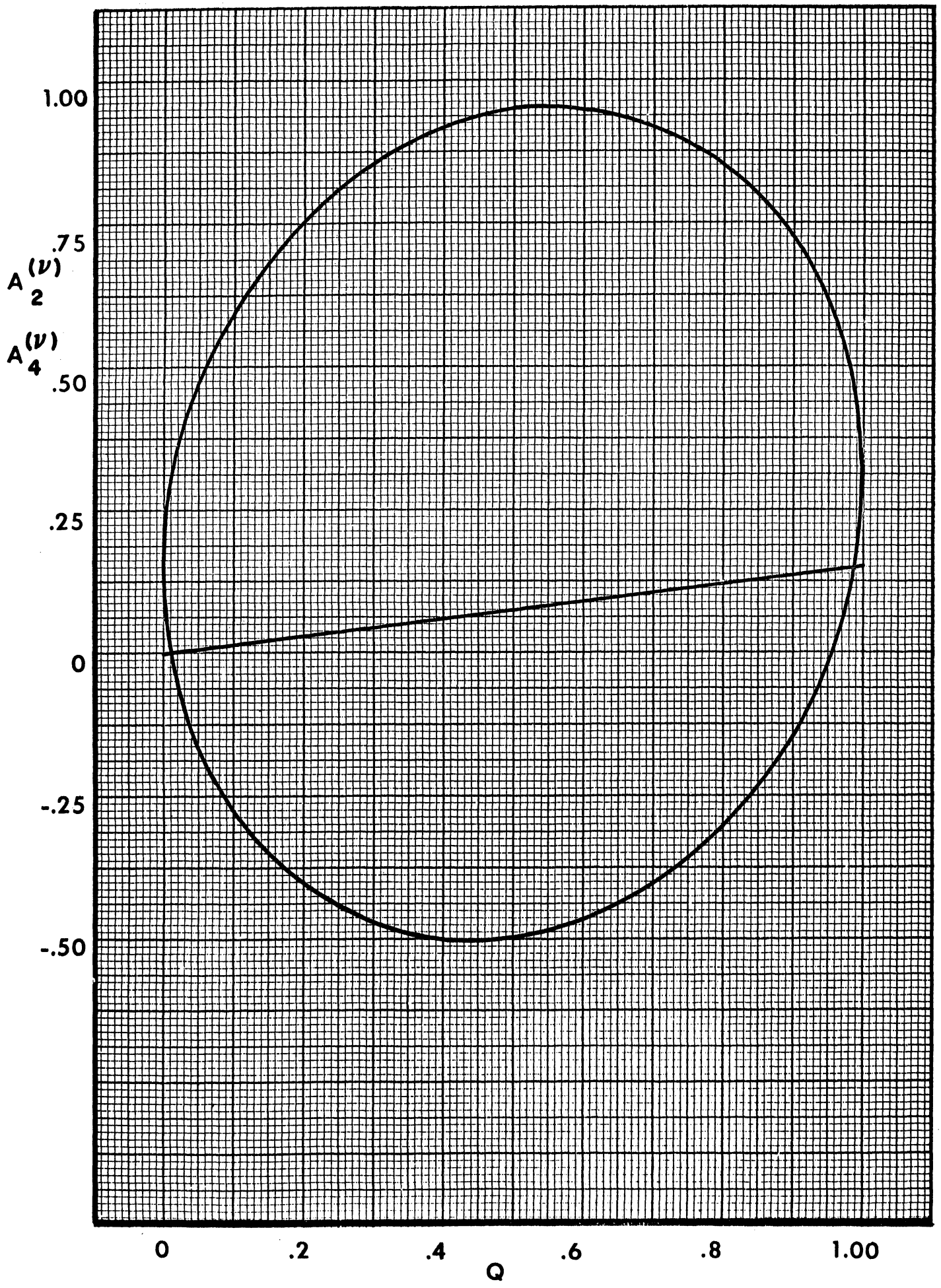
3(D,Q) 4
J = 3, J' = 4
1.00
.75
$A_2^{(\nu)}$
$A_4^{(\nu)}$
.50
.25
0
-.25
-.50
0
.2
.4
.6
.8
1.00
Q

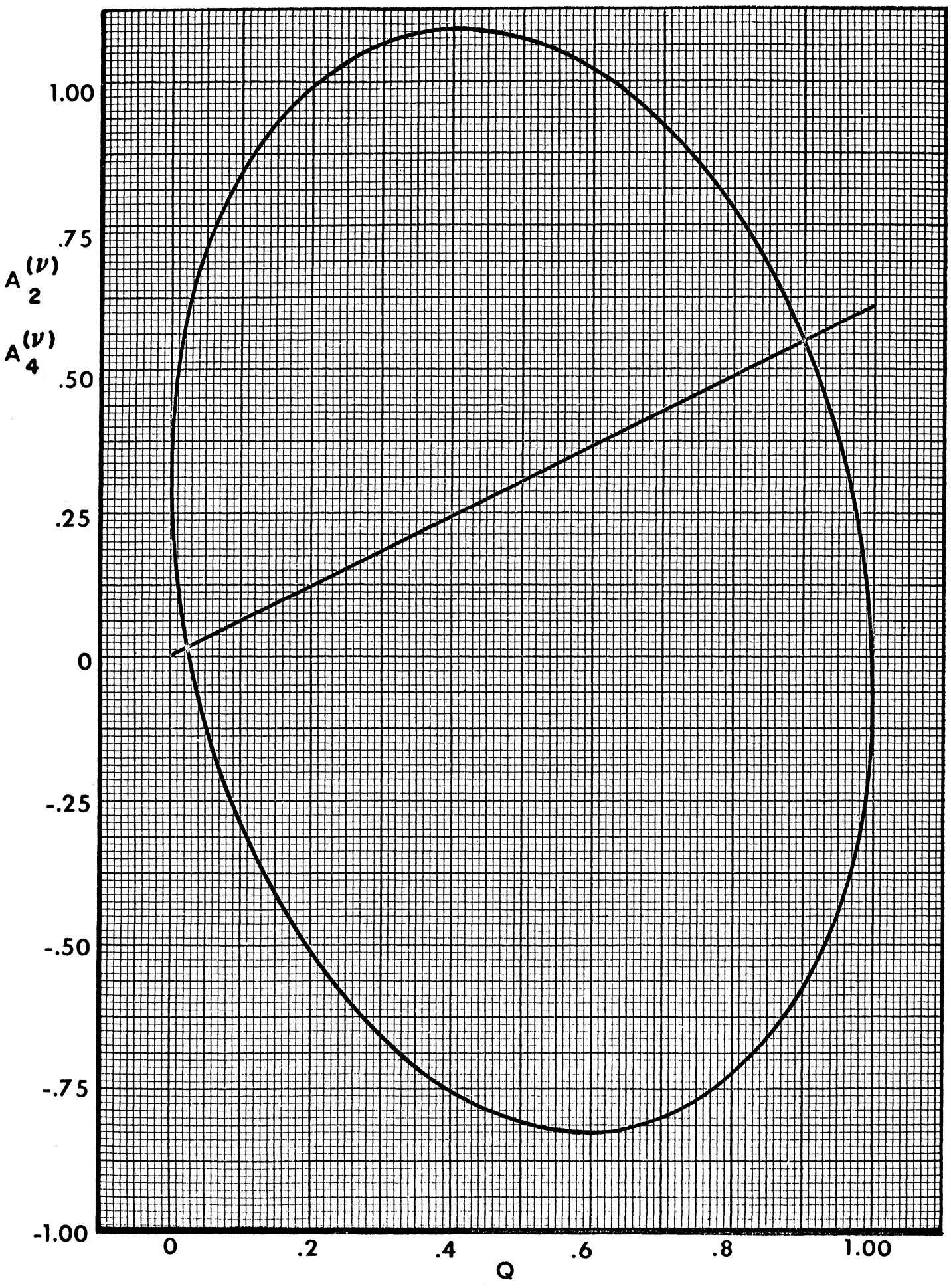
4 (D,Q) 3
J = 4, J' = 3
1.00
.75
$A_2^{(\nu)}$
$A_4^{(\nu)}$
.50
.25
0
-.25
-.50
-.75
-1.00
0
.2
.4
.6
.8
1.00
Q

4 (D,Q) 4

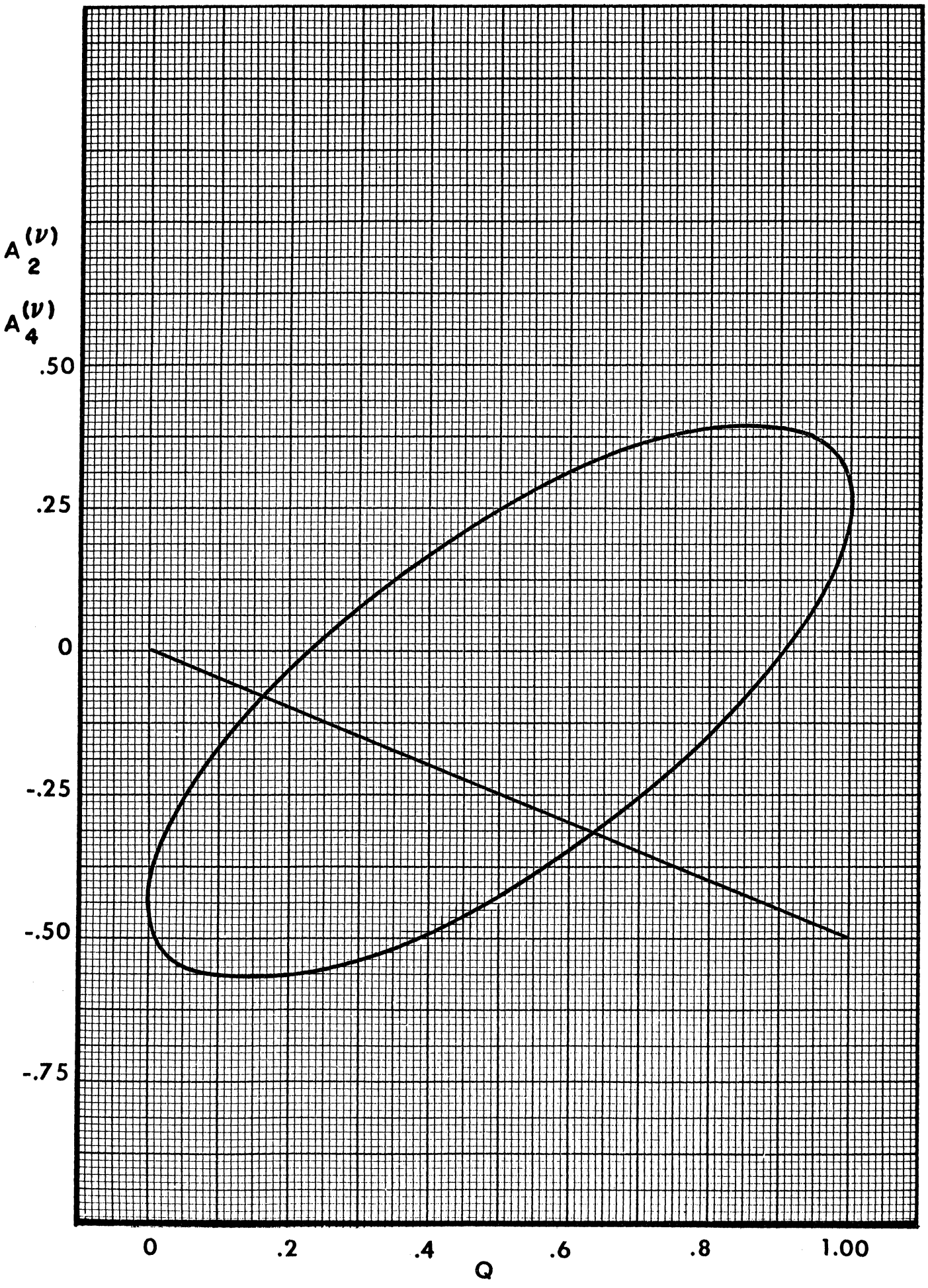

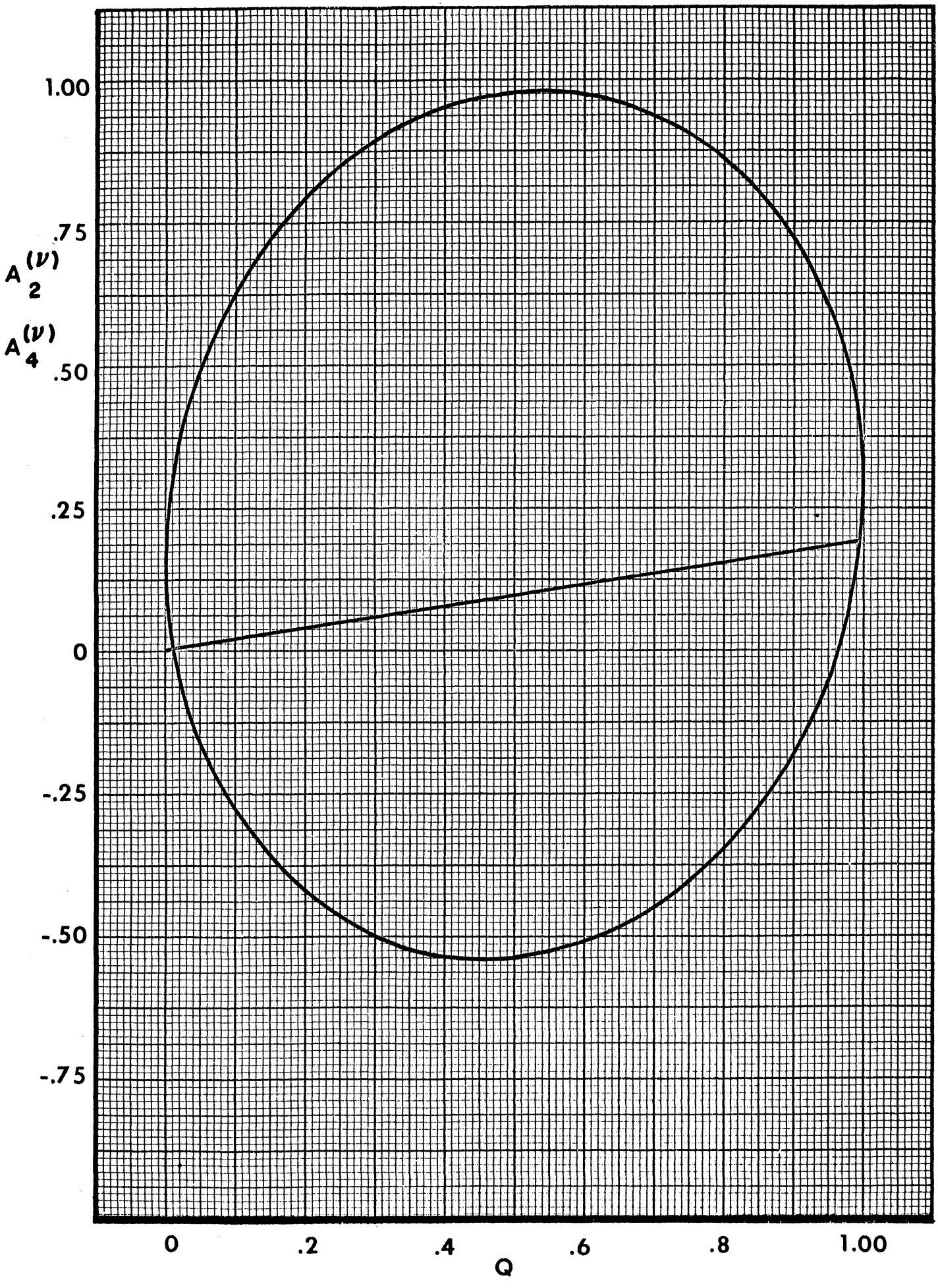
4 (D,Q) 5
J = 4, J' = 5
1.00
.75
$A_2^{(\nu)}$
$A_4^{(\nu)}$
.50
.25
0
-.25
-.50
-.75
0
.2
.4
.6
.8
1.00
Q

5 (D,Q) 4

J = 5, J' = 4

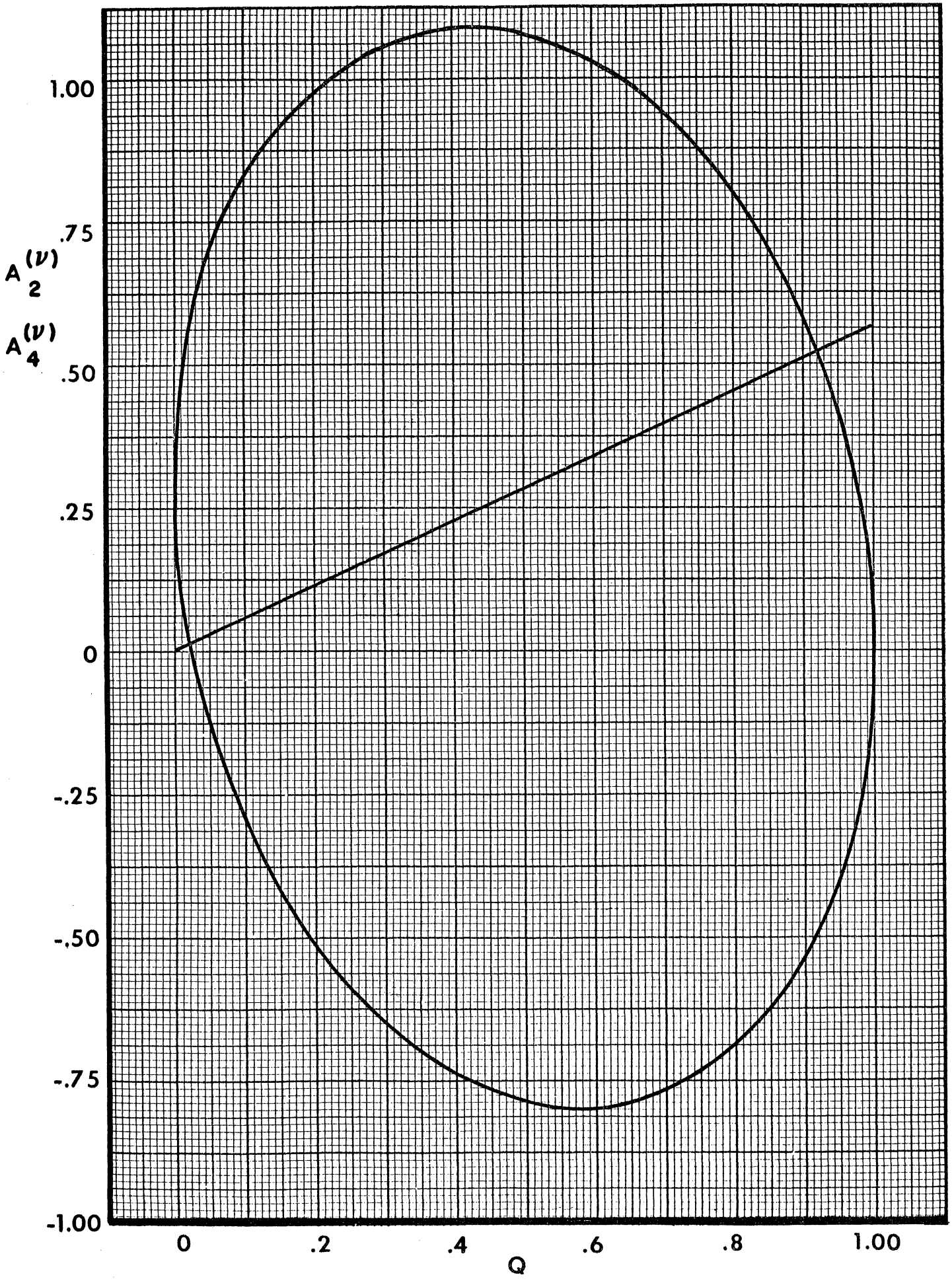

5 (D,Q) 5

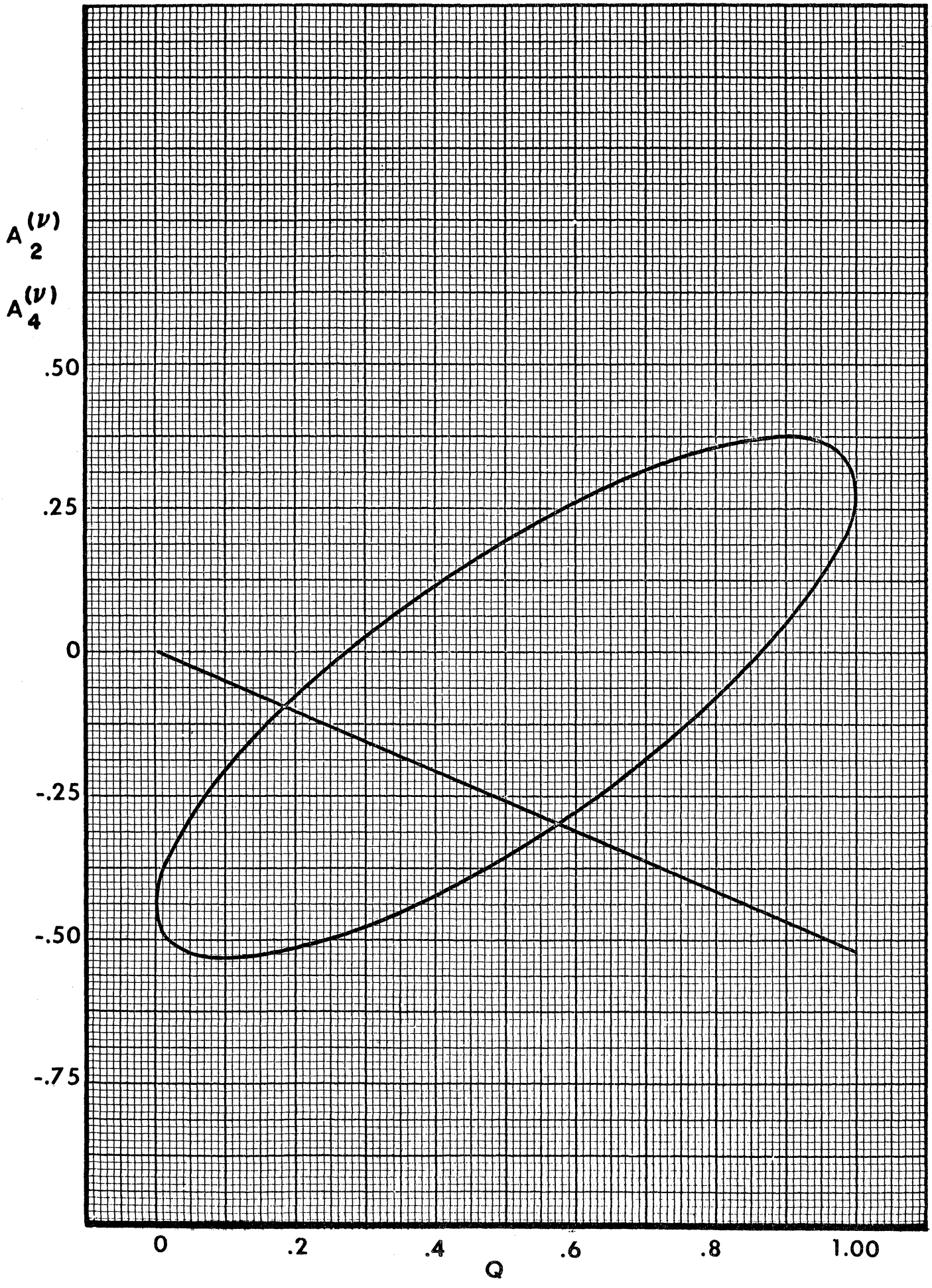

5 (D,Q) 6

J = 5, J' = 6

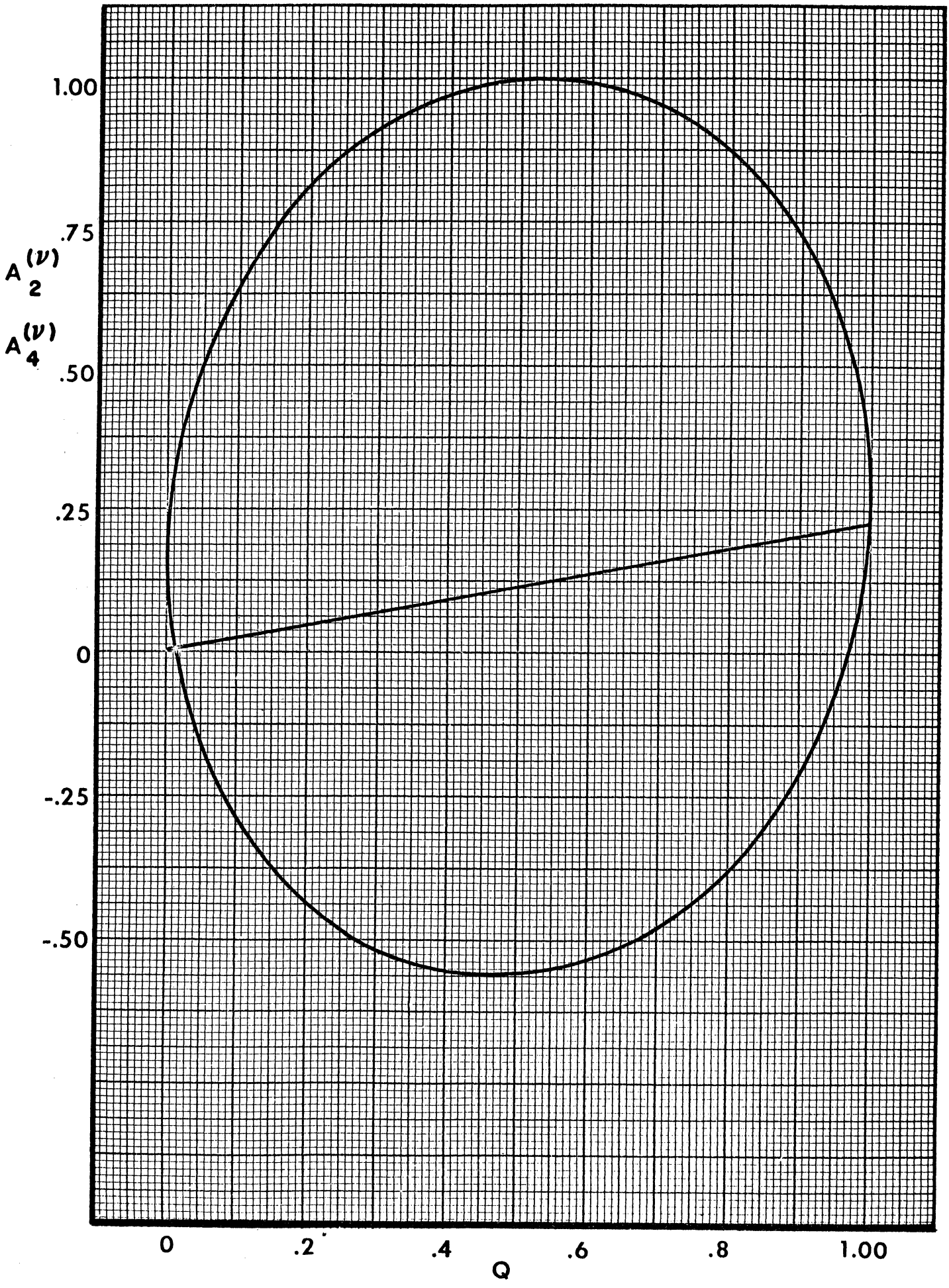

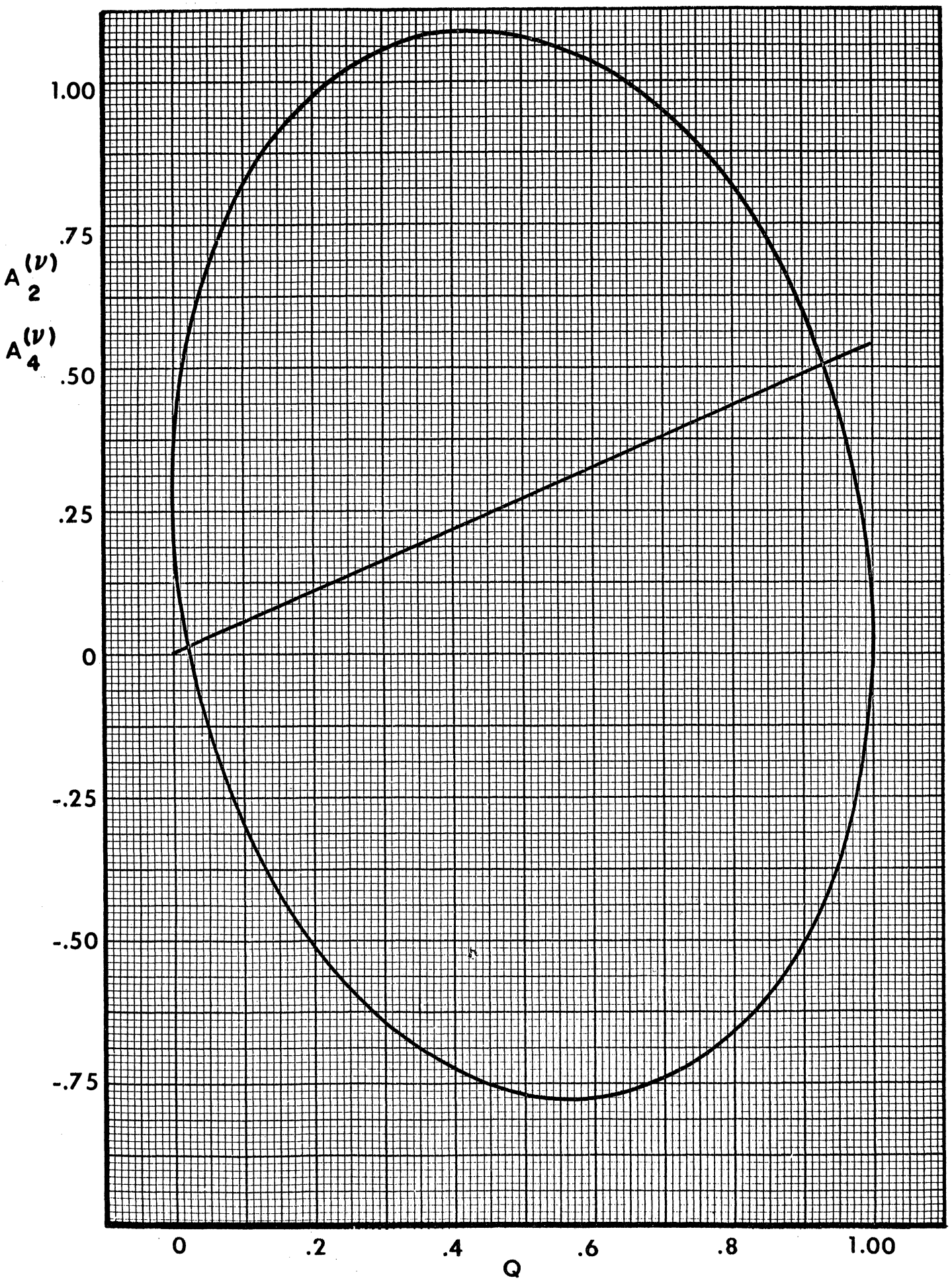
6 (D,Q) 5
J = 6, J' = 5
1.00
.75
$A_2^{(\nu)}$
$A_4^{(\nu)}$
.50
.25
0
-.25
-.50
-.75
0
.2
.4
.6
.8
1.00
Q

6 (D,Q) 6

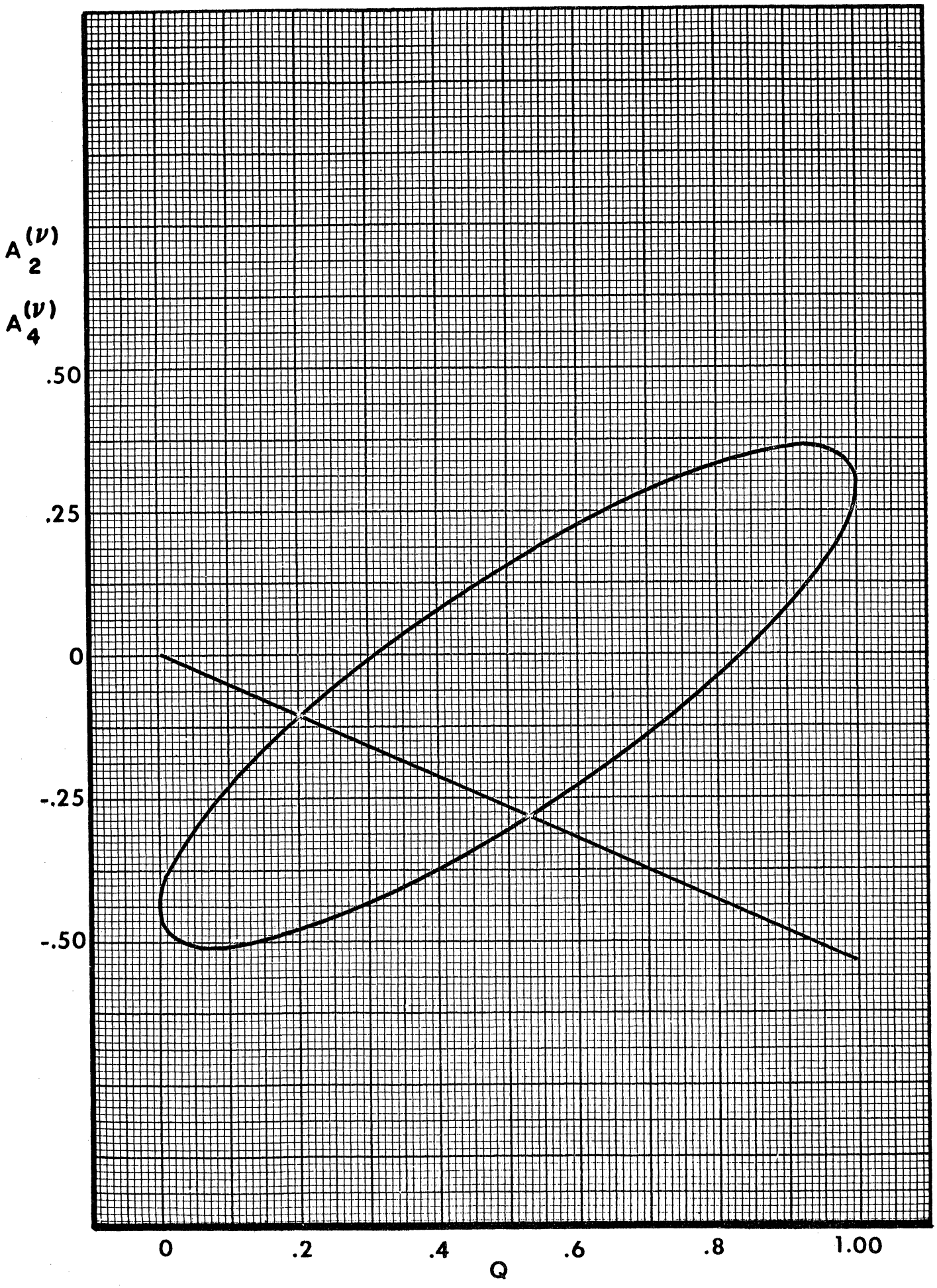

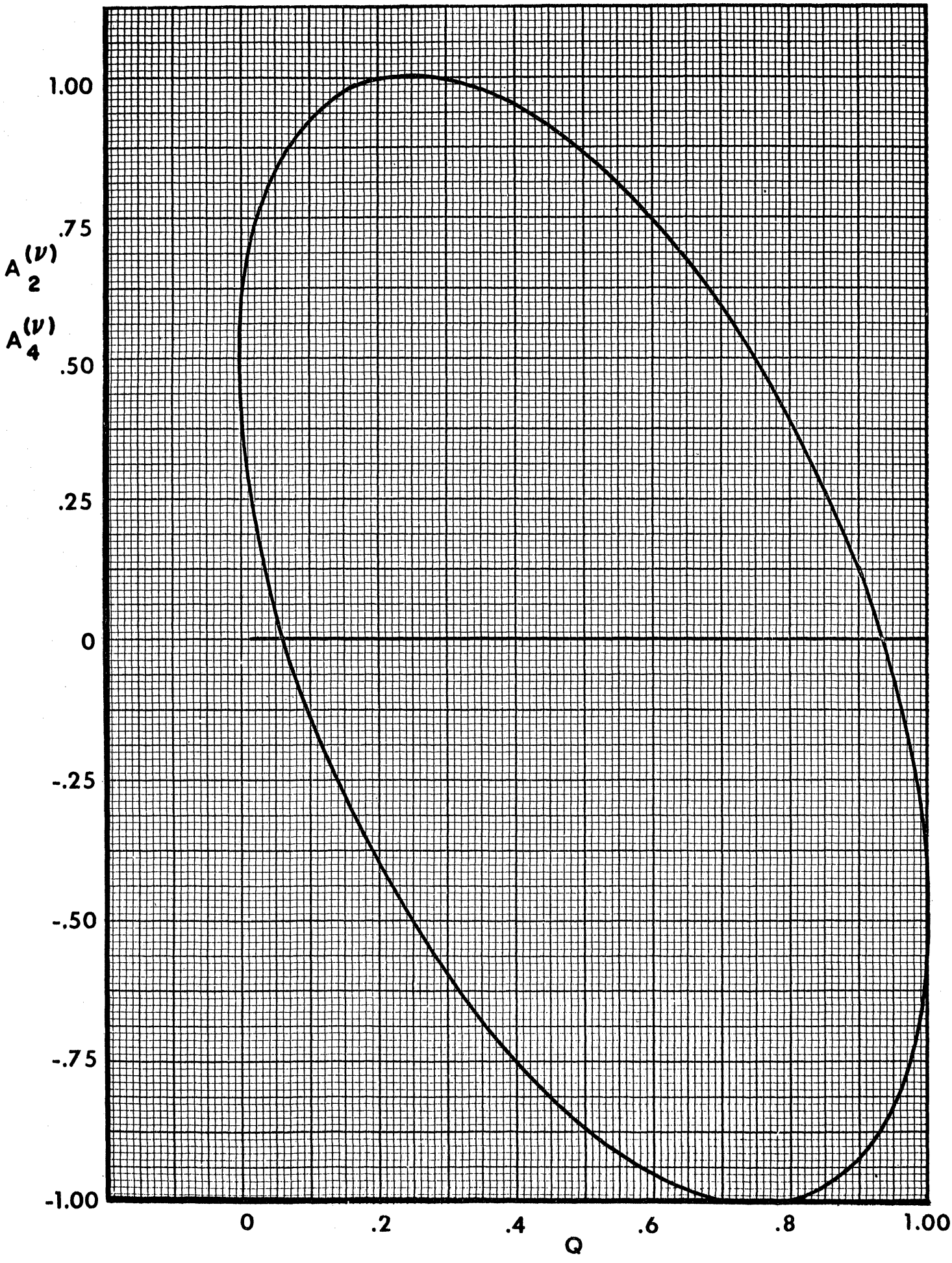
3 / 2 (D,Q) 1 / 2
J = 3 / 2, J' = 1 / 2
1.00
.75
$A_2^{(\nu)}$
$A_4^{(\nu)}$
.50
.25
0
-.25
-.50
-.75
-1.00
0
.2
.4
.6
.8
1.00
Q

3 / 2 (D,Q) 3 / 2

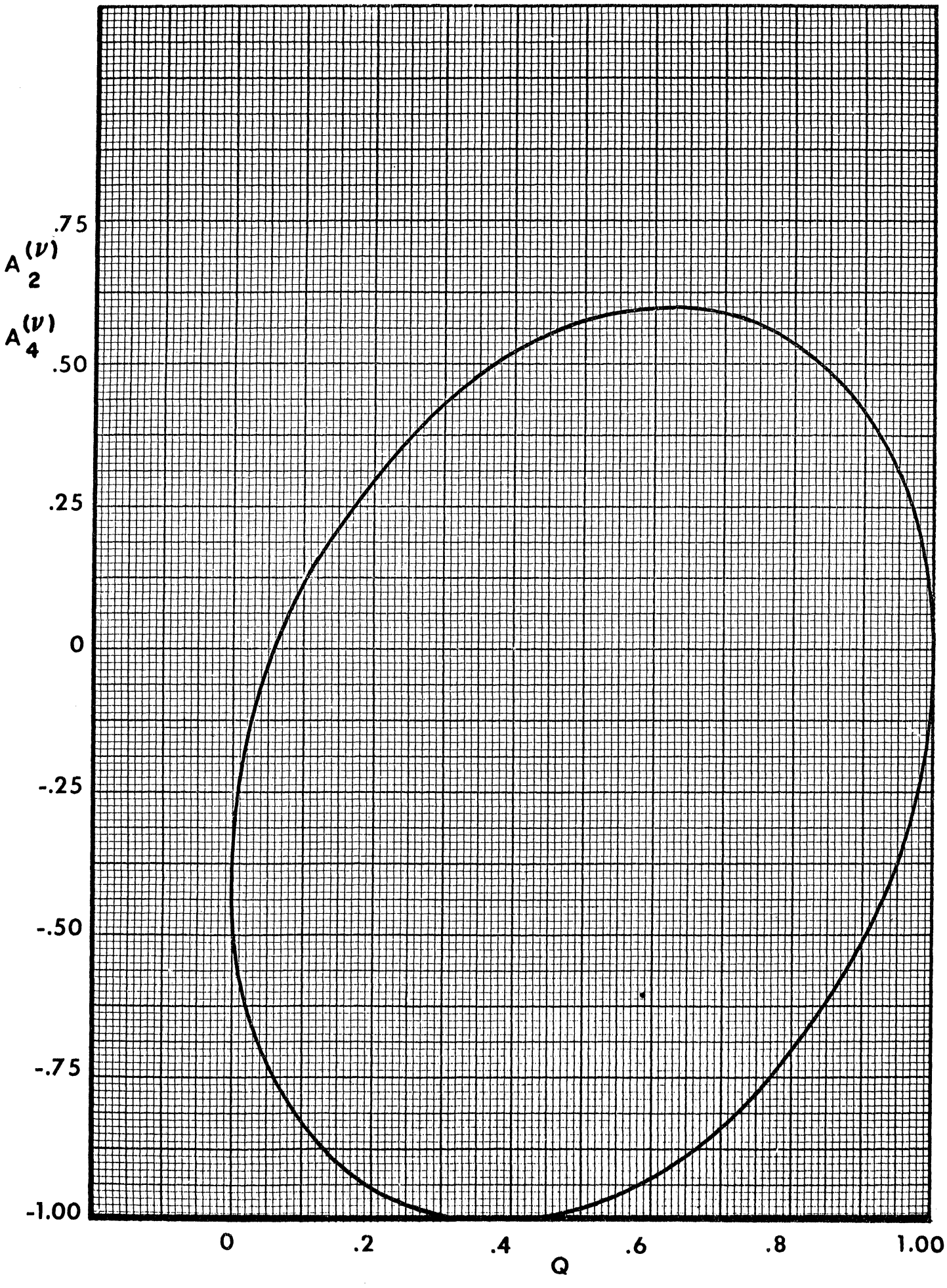

3 / 2 (D,Q) 5 / 2

J = 3 / 2, J' = 5 / 2

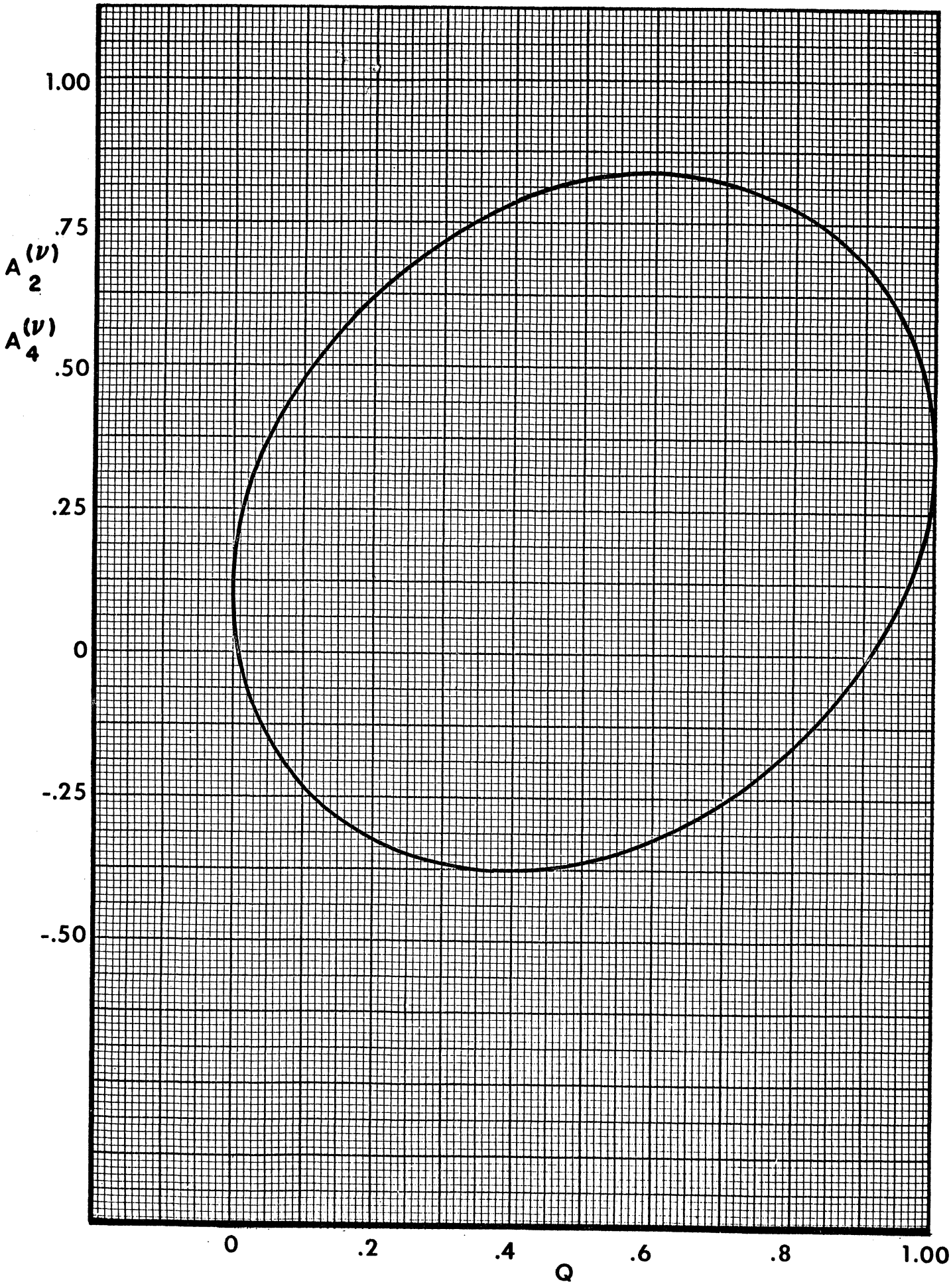

5 / 2 (D,Q) 3 / 2

J = 5 / 2, J' = 3 / 2

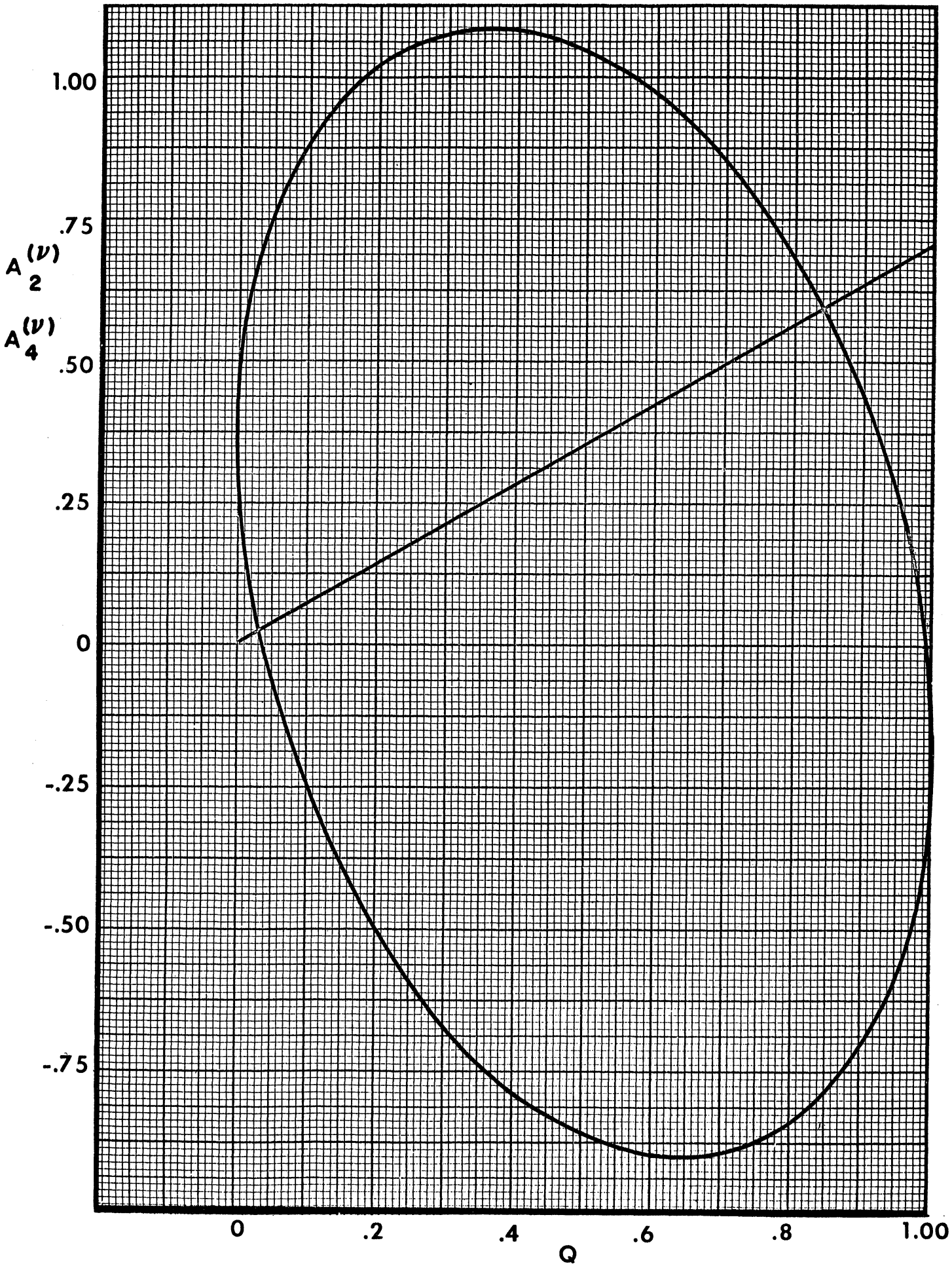

5 / 2 (D,Q) 5 / 2

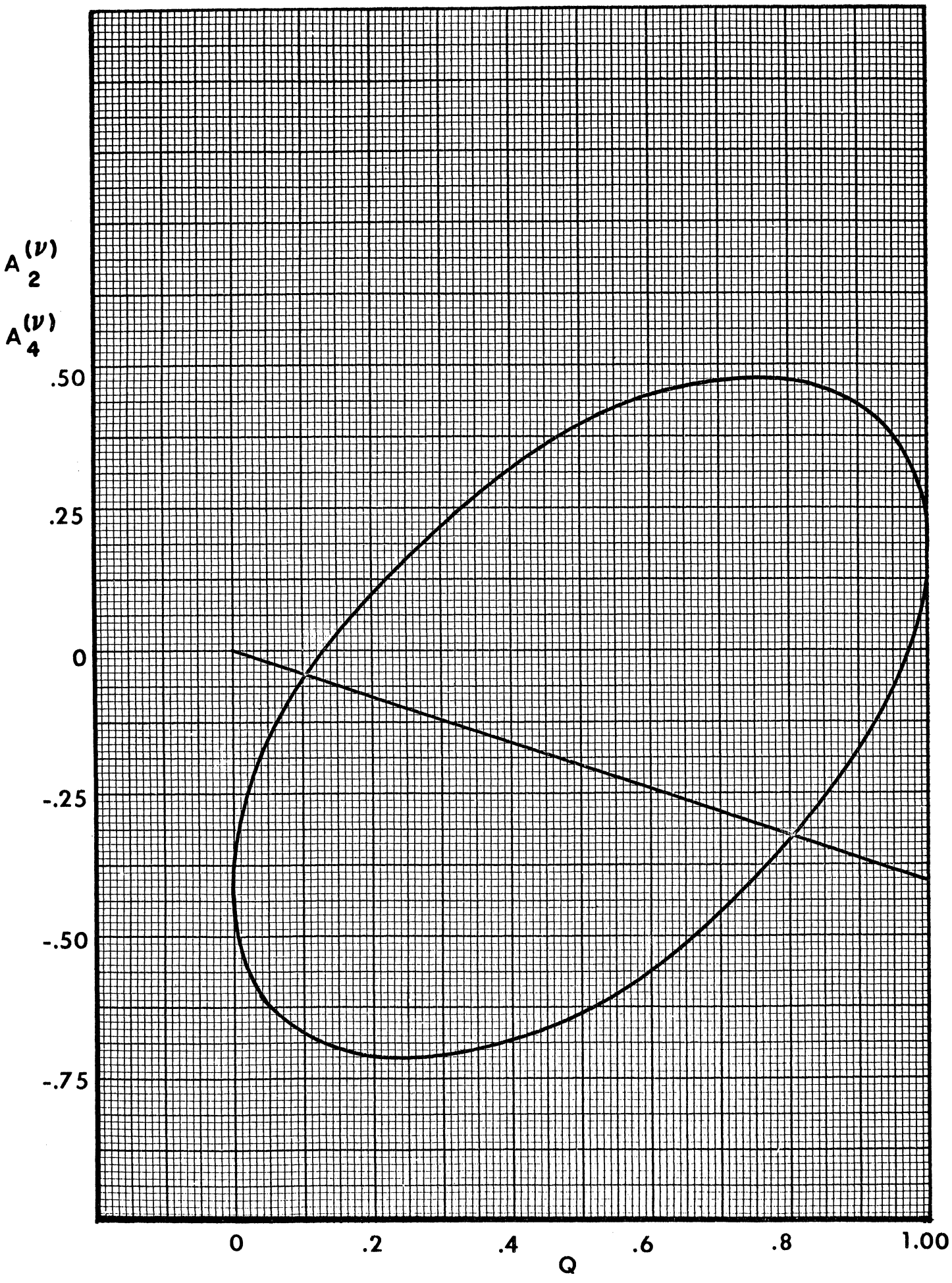

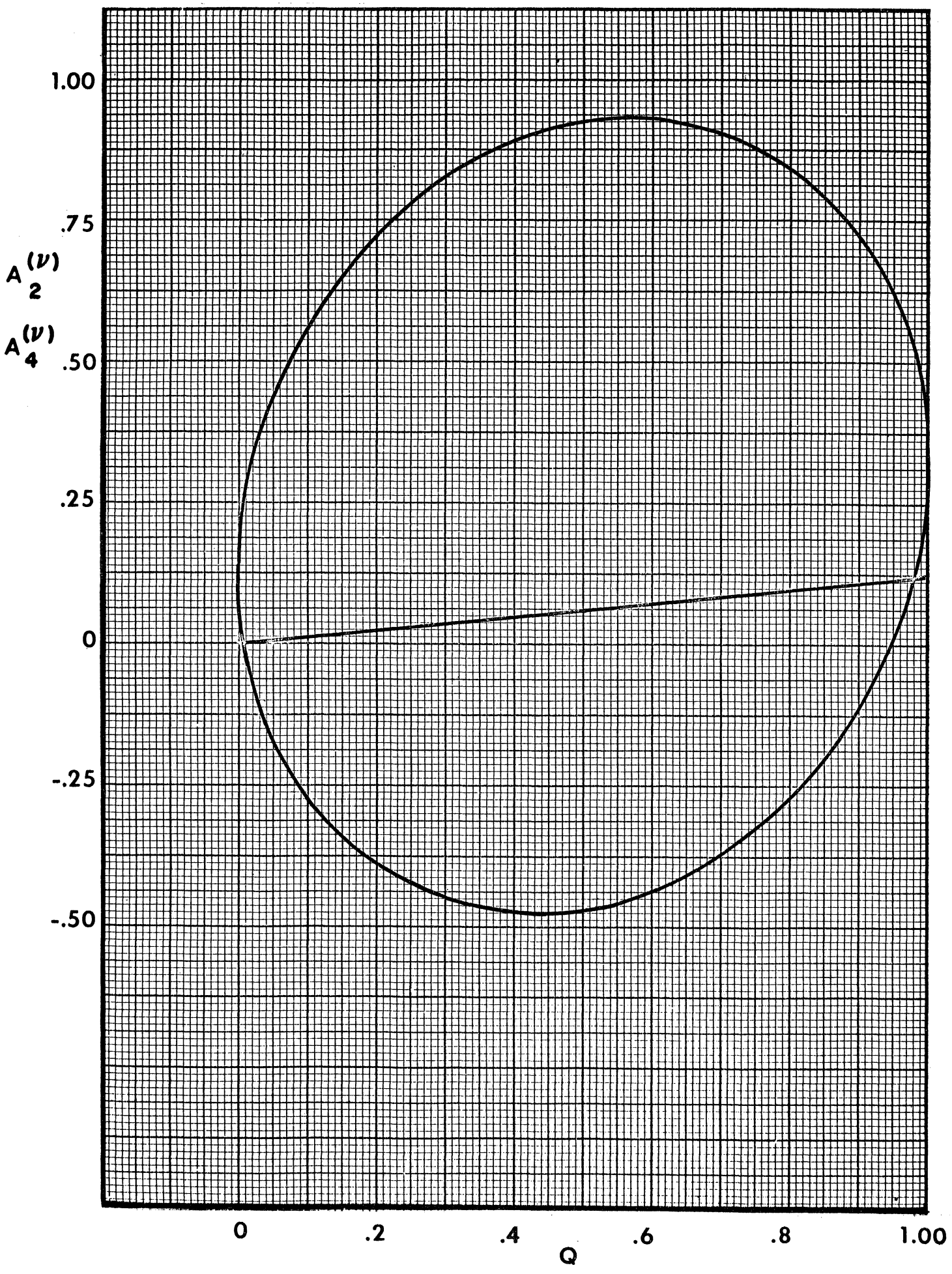
5 / 2 (D,Q) 7 / 2
J = 5 / 2, J' = 7 / 2
1.00
.75
$A_2^{(\nu)}$
$A_4^{(\nu)}$
.50
.25
0
-.25
-.50
0
.2
.4
.6
.8
1.00
Q

7 / 2 (D,Q) 5 / 2

J = 7 / 2, J' = 5 / 2

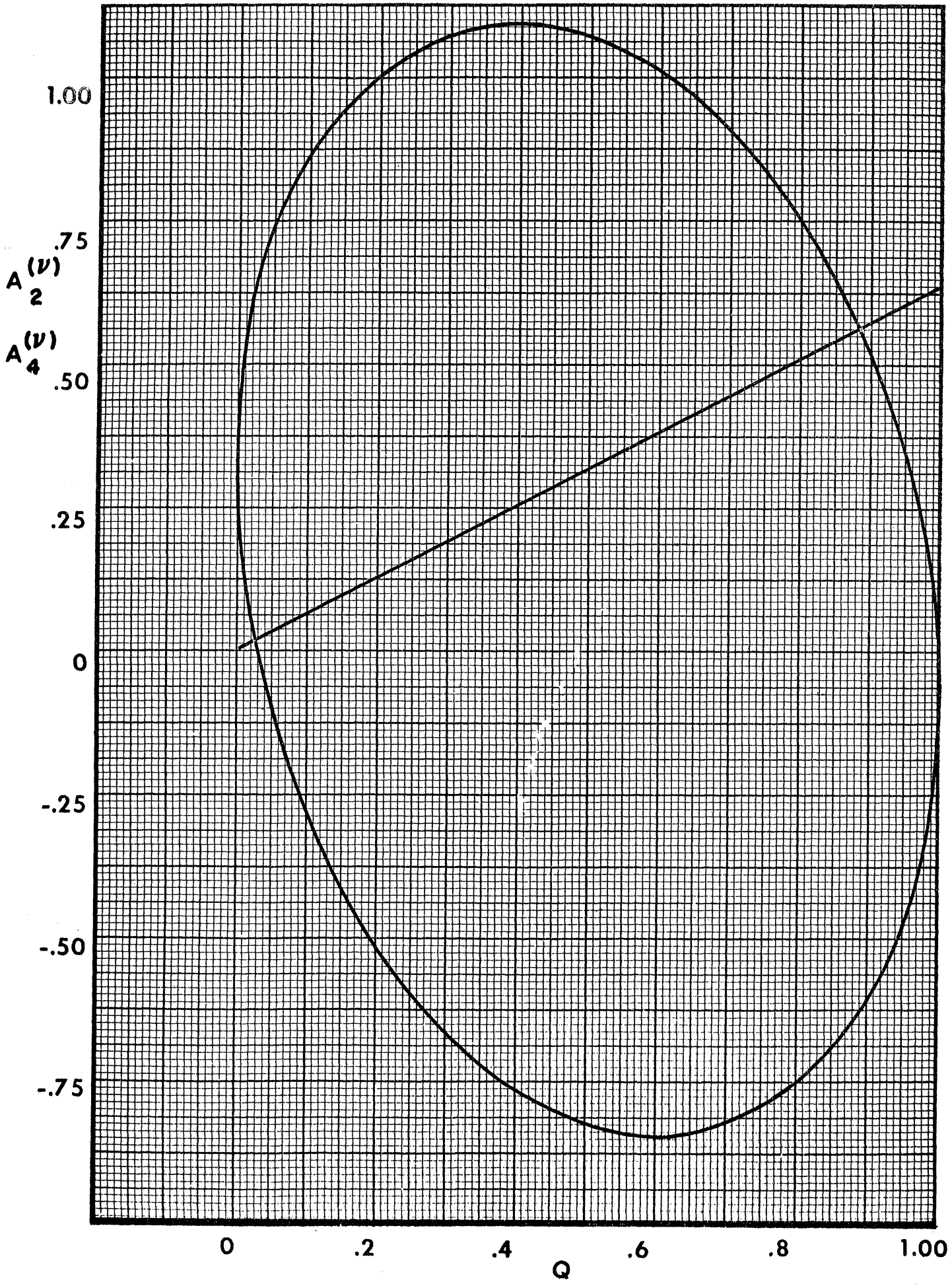

7 / 2 (D,Q) 7 / 2

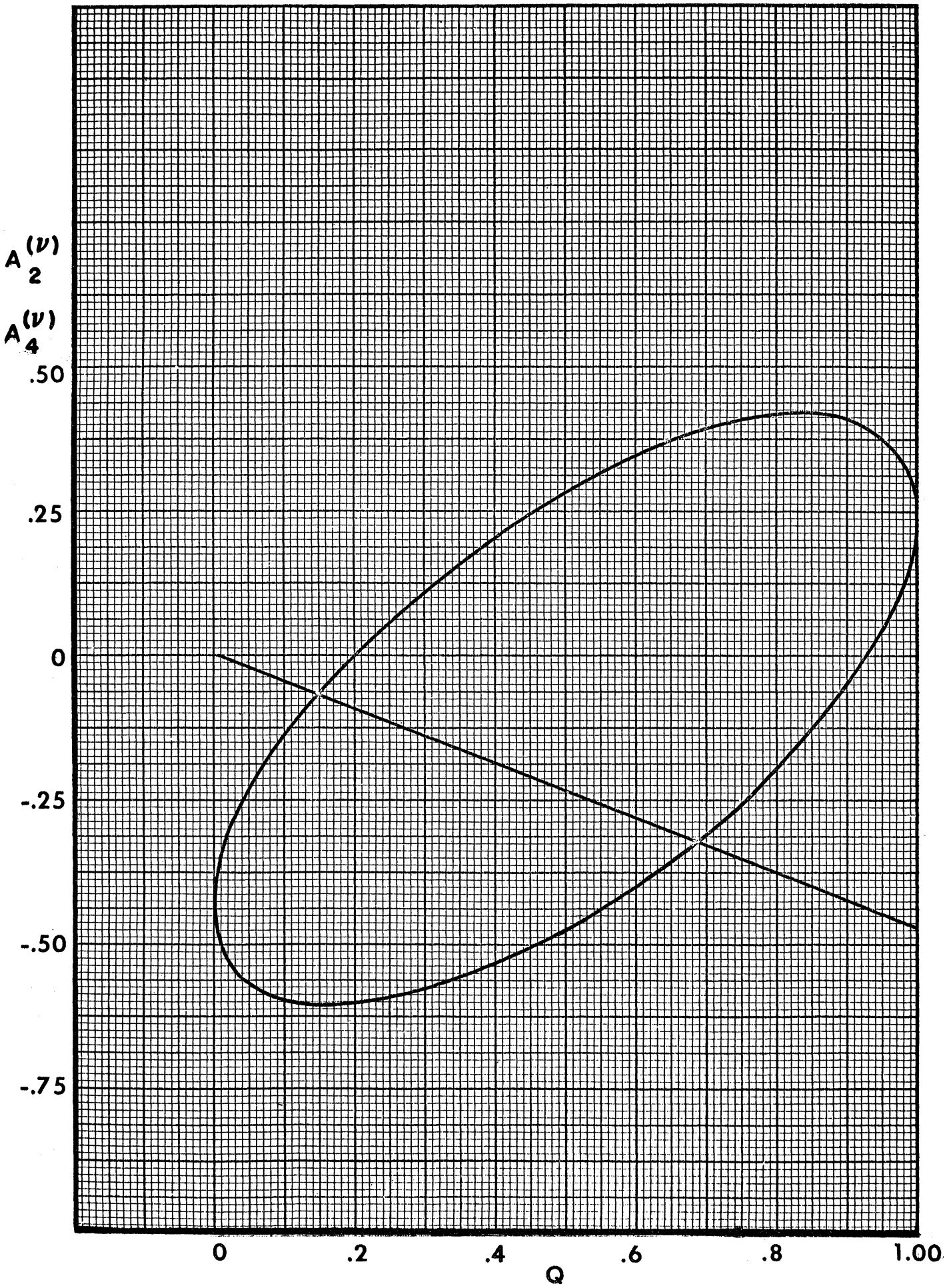

7 / 2 (D,Q) 9 / 2

J = 7 / 2, J' = 9 / 2

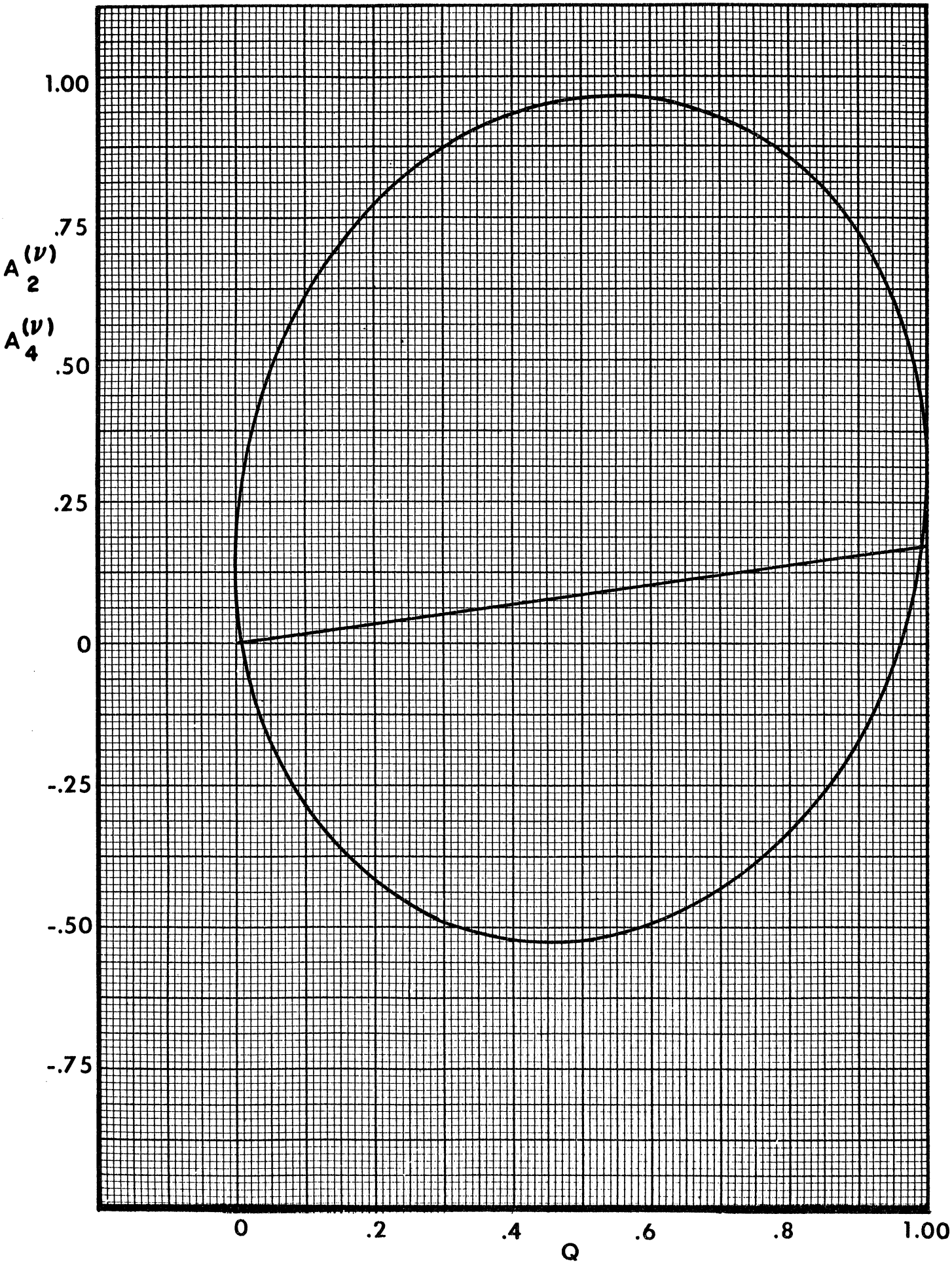

9 / 2 (D,Q) 7 / 2

J = 9 / 2, J' = 7 / 2

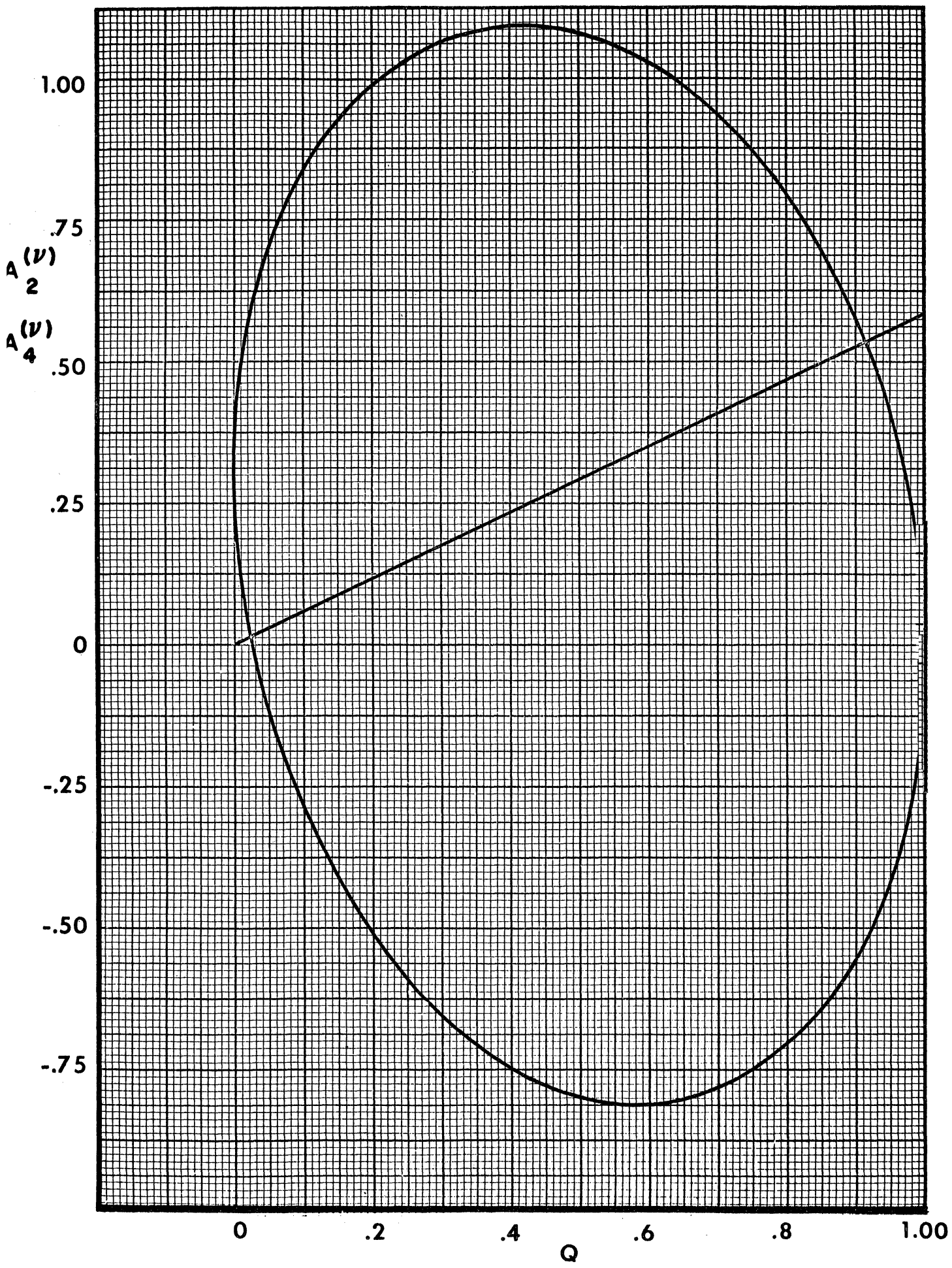

9/2 (D,Q) 9/2

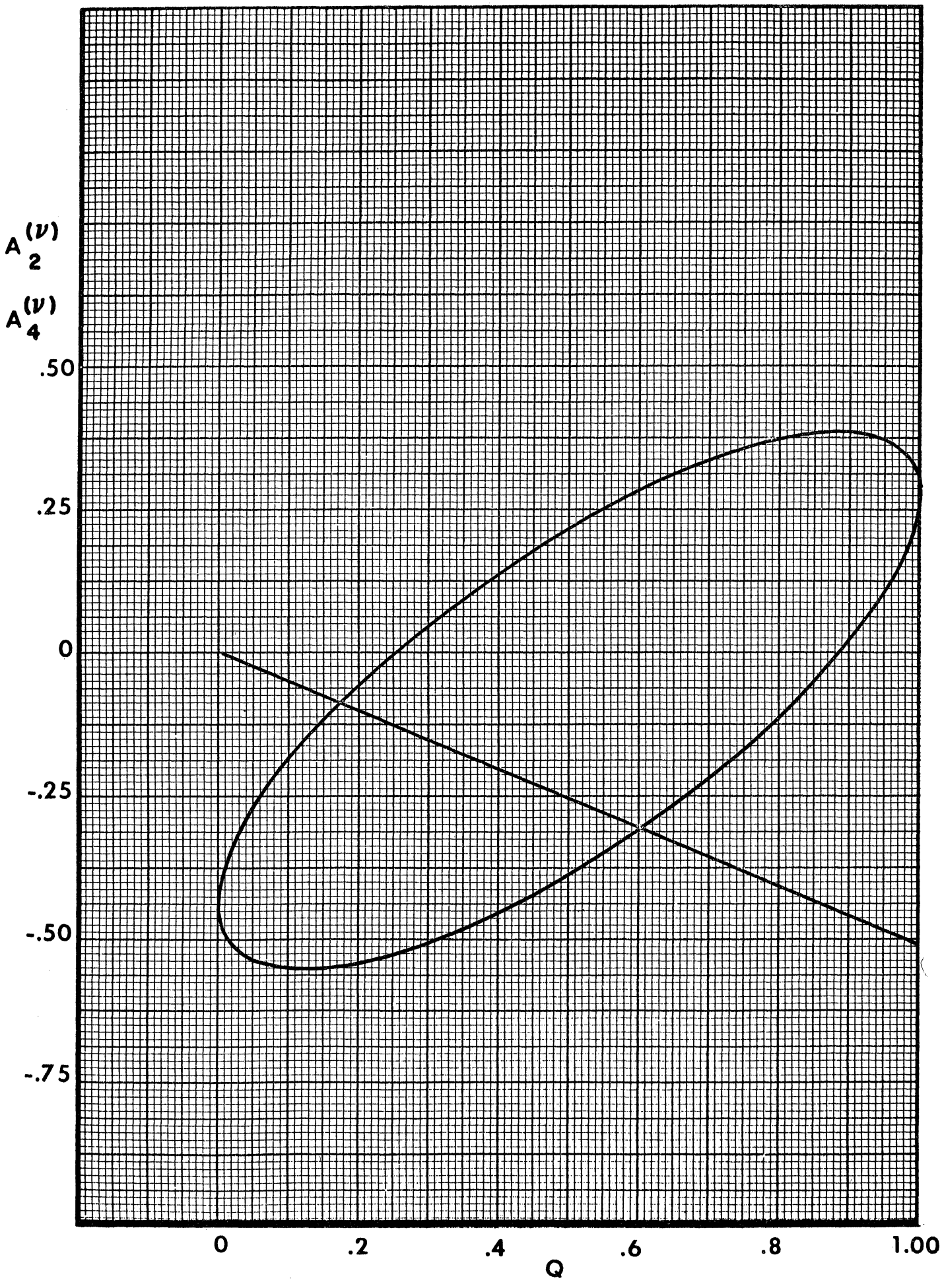

9/2 (D,Q) 11/2

J=9/2, J'=11/2